A radio 269 ms radio pulsar in the gamma-ray binary LS I +61° 303

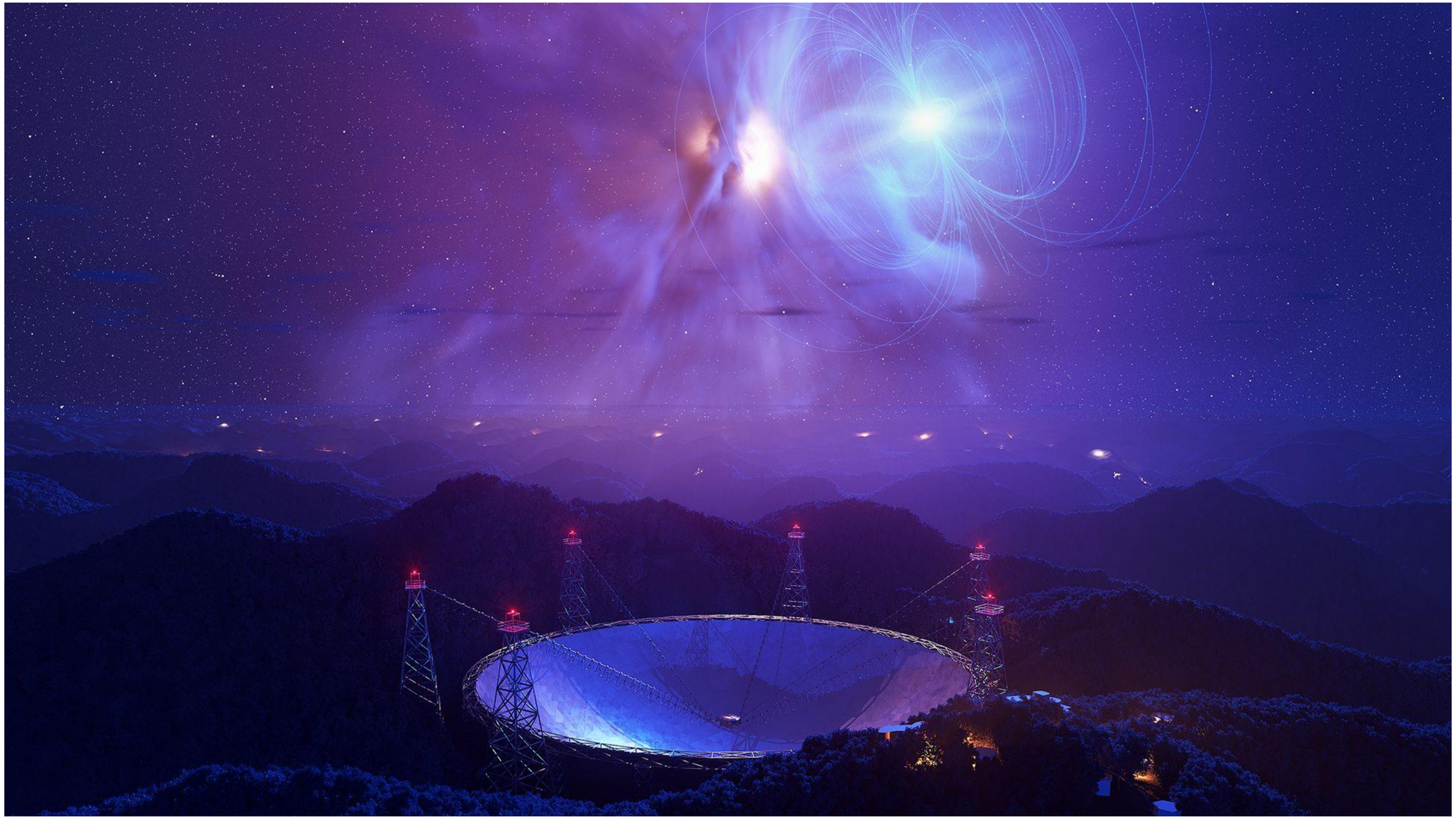

Alessandro Papitto – INAF OA Roma

11/5/2022 – INAF IASF Milan

nature astronomy

LETTERS

https://doi.org/10.1038/s41550-022-01630-1

Check for updates

Radio pulsations from a neutron star within the gamma-ray binary LS I +61° 303

Shan-Shan Weng[1,14] ✉, Lei Qian[2,3,14], Bo-Jun Wang[2,4,5,14], D. F. Torres[6,7,8] ✉, A. Papitto[9], Peng Jiang[2,3], Renxin Xu[4,5], Jian Li[10,11], Jing-Zhi Yan[12], Qing-Zhong Liu[12], Ming-Yu Ge[13] and Qi-Rong Yuan[1]

LS I +61° 303 hosts a **young, highly magnetised NS with magnetar behavior**

Gamma-ray binaries are **pulsar wind nebulae in a binary environment**

Gamma-ray binaries are **progenitors of high mass X-ray binaries**

Gamma-ray binaries

Massive star + compact object.

Emission peaks above 0.1 GeV

Particle acceleration in a binary system

Accretion-powered **microquasars**
vs
rotation-powered **pulsars**

Black holes vs **Neutron Stars**

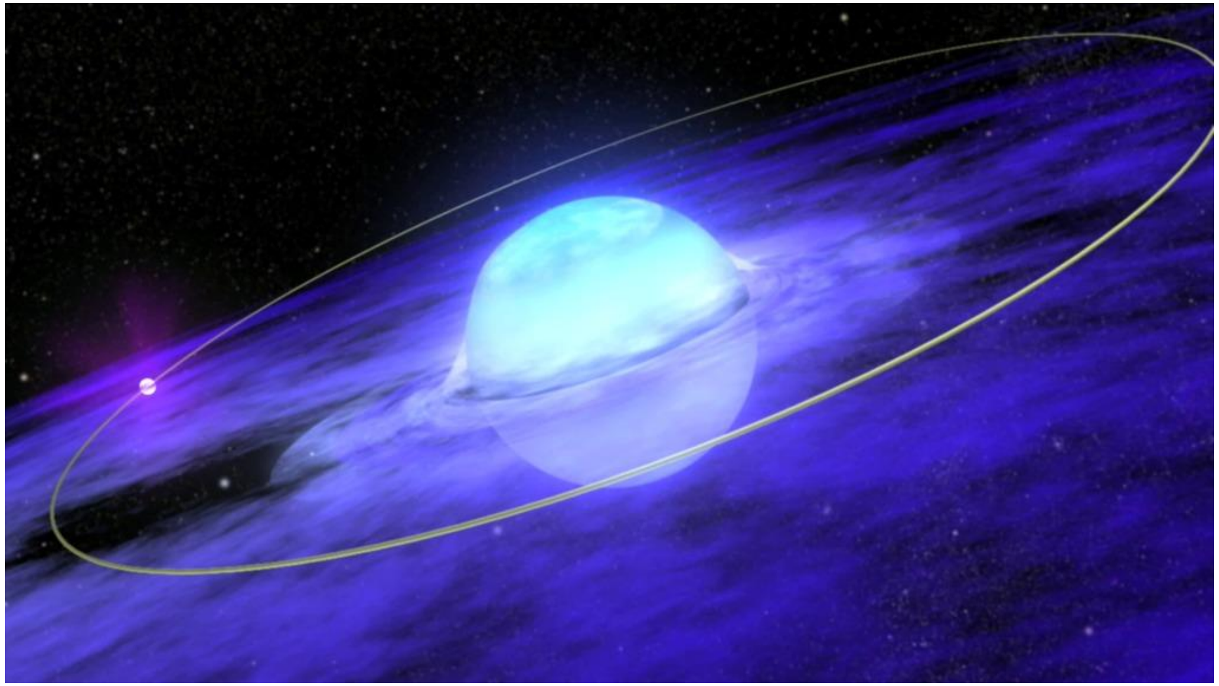

Gamma-ray binaries

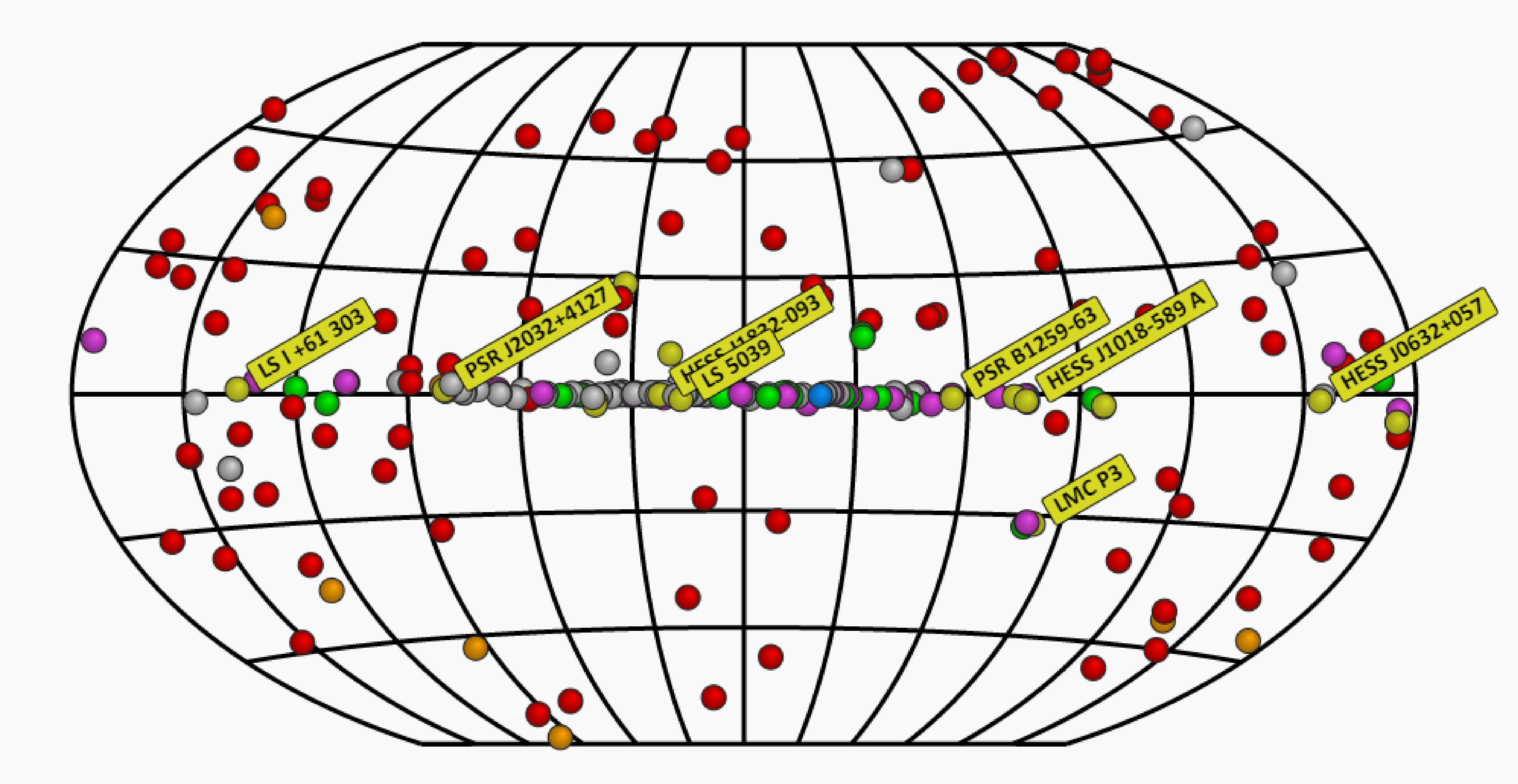

LS I +61 303 spectral energy distribution

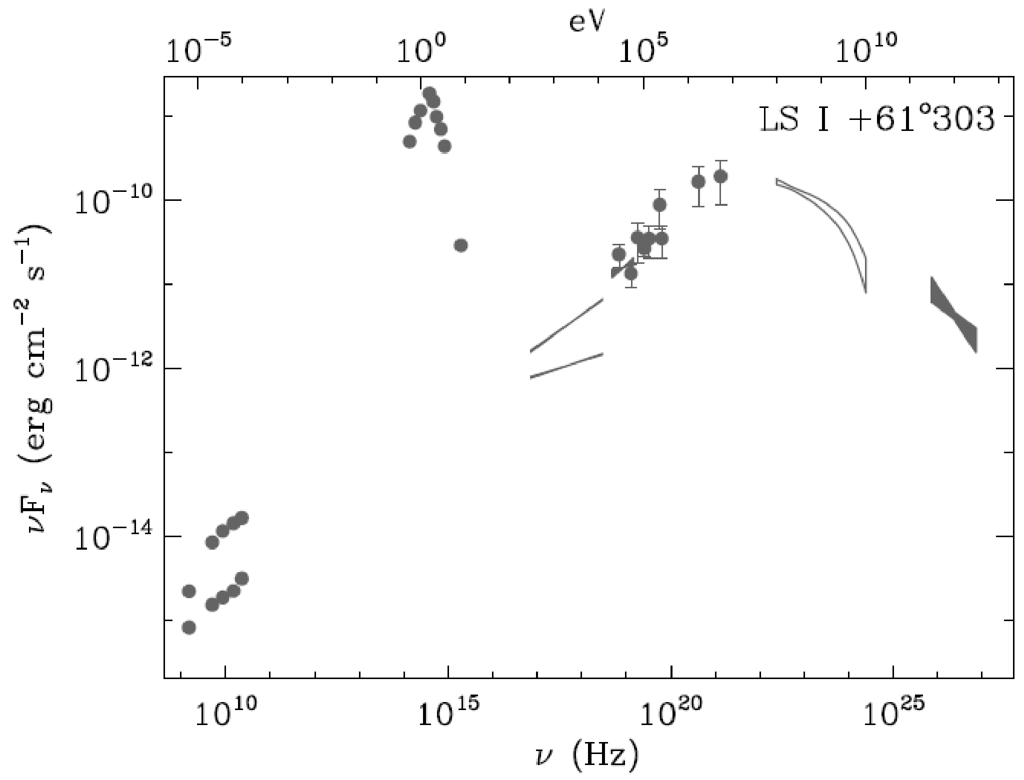

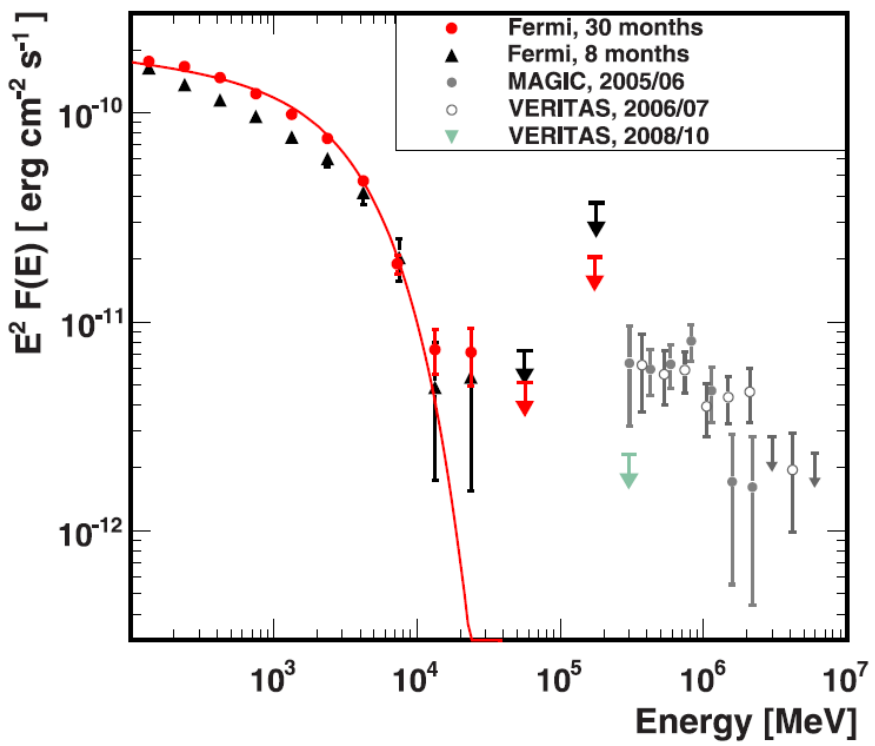

$L_{VHE} \approx L_{Xray}$ 0.14 x 10^{35} erg/s
$L_{HE} \approx$ 2.8 x 10^{35} erg/s

Synchrotron (X-rays) + Inverse Compton (γ-rays)

Dubus 2013

Hadasch+ 2012

Orbital modulation
at all energies

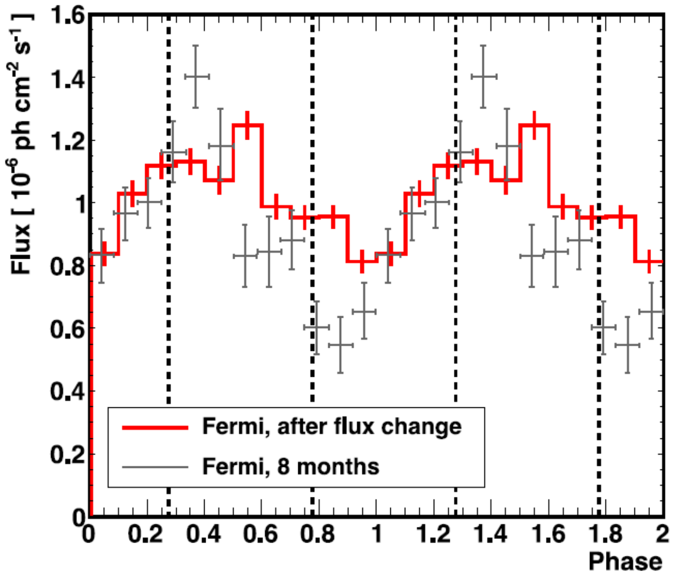

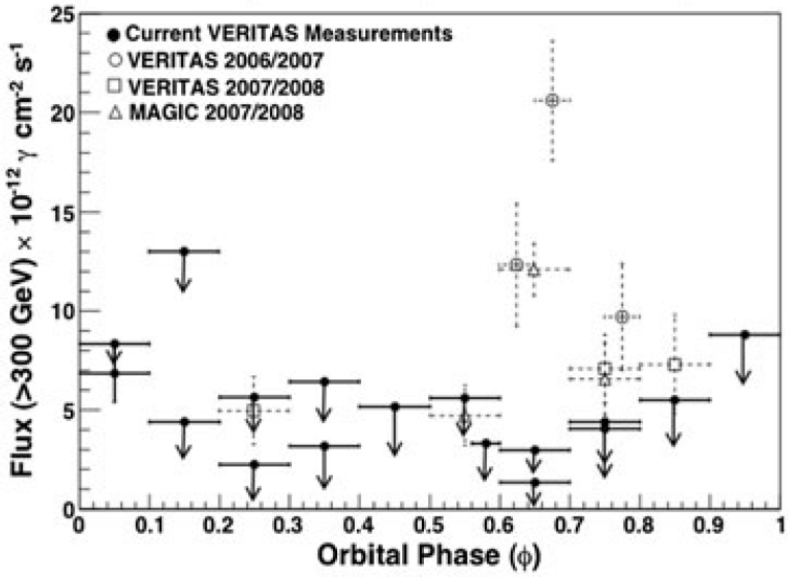

LS I +61° 303

P_{orb} = 24.5 days

Superorbital variability = 4.5 years

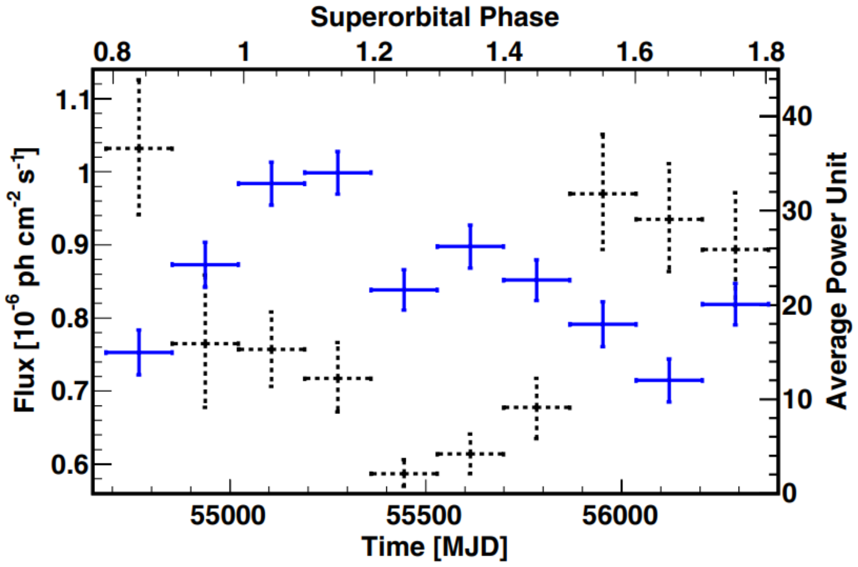

Gamma-ray binaries

Massive stellar companion

M_2 = 10-30 $M_\odot$

O/Be type

Porb = 4 days –40 years

Eccentricity = 0.5-0.9

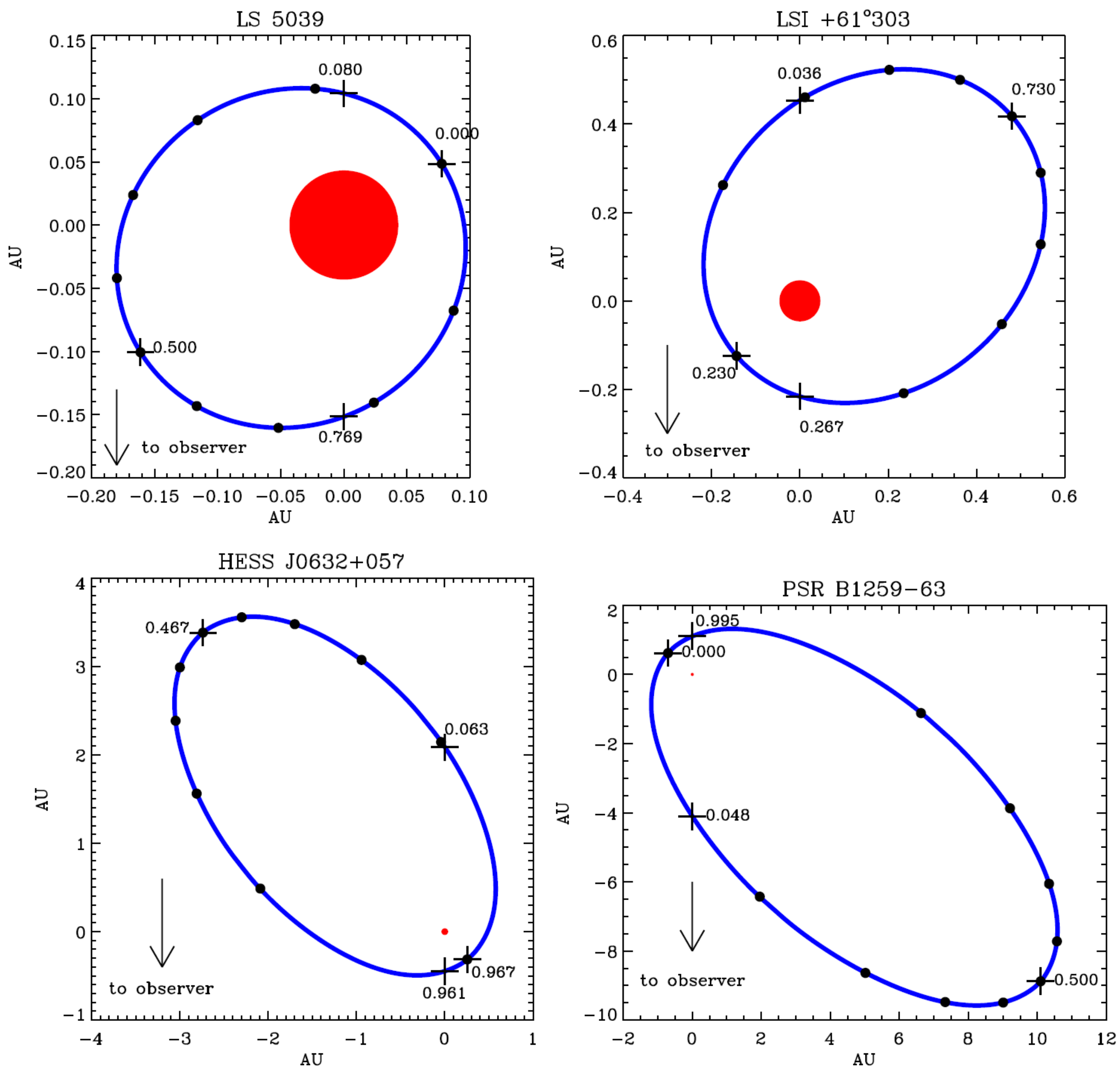

Dubus 2013

High mass Gamma-ray binaries (vs HMXBs)

Emission peaks above 0.1 GeV. Also VHE sources.

Orbital modulation at all wavelengths

Radio emission

Relatively faint in X-rays. Hard X-ray spectra with no cut-off. No X-ray pulses.

What is the nature of the compact object?

What powers particle acceleration?

Pulsar wind nebula in a binary

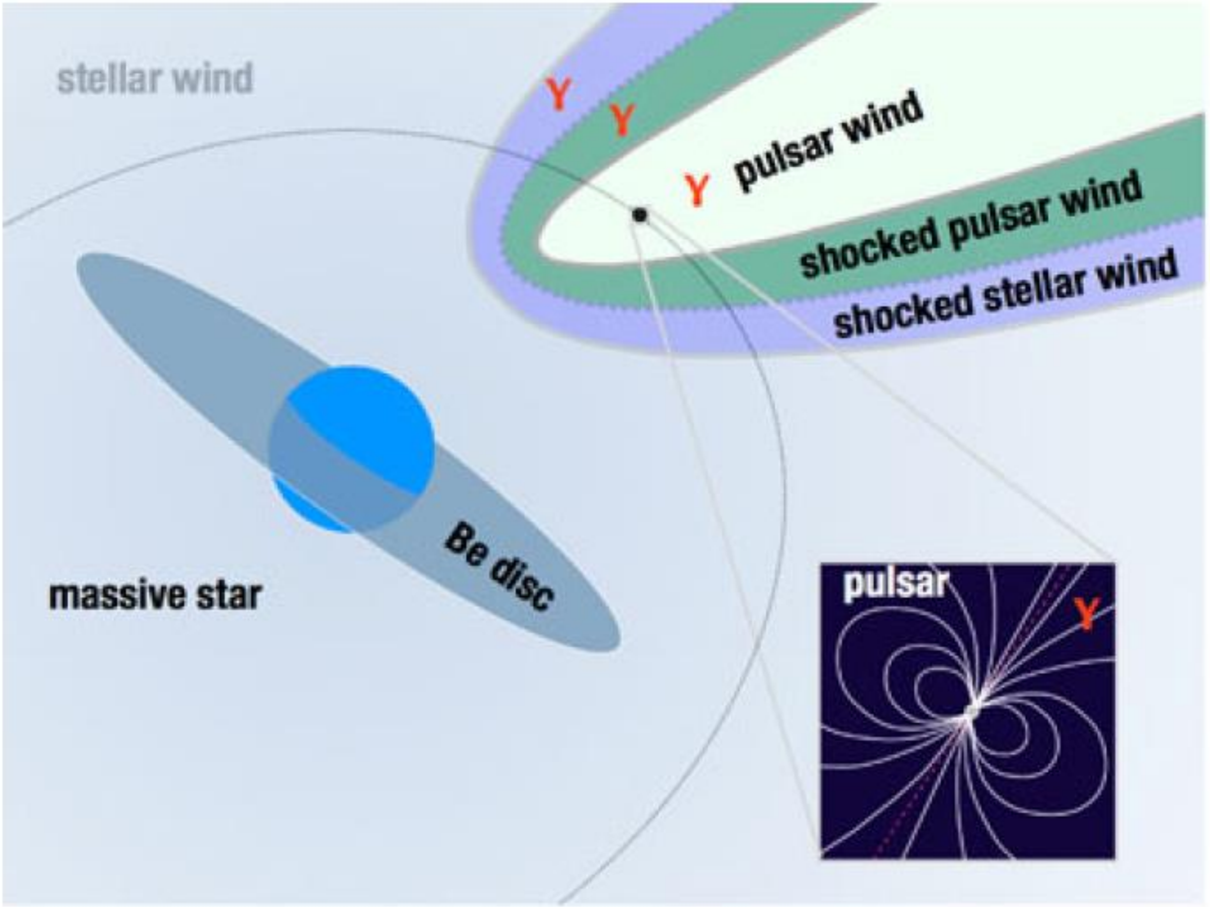

Particle acceleration at the shock
and/or pulsar magnetosphere and wind

Accreting microquasar

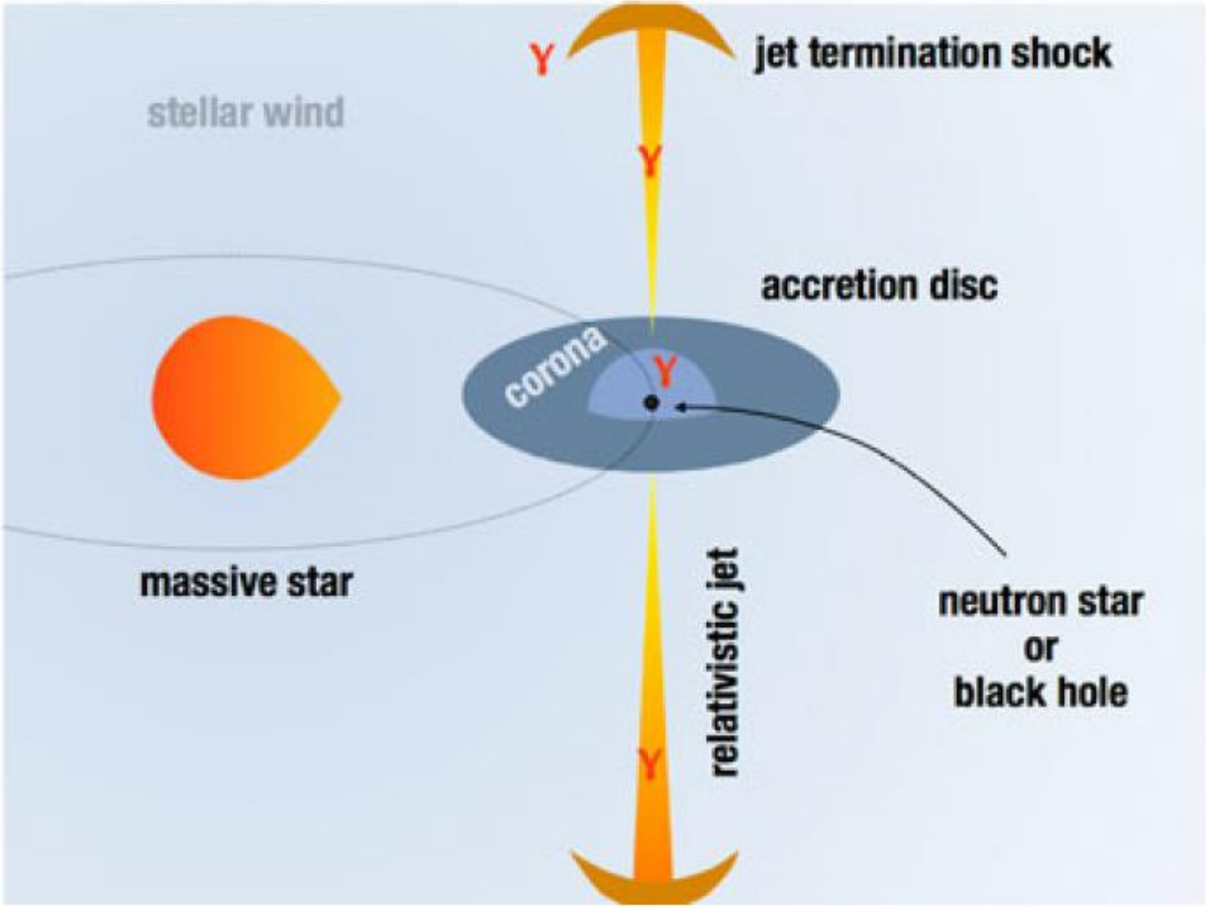

Corona, Relativistic jet and/or jet
termination shock

Only two gamma-ray binaries detected as radio pulsars (so far)

PSR B1259+63 Pspin = 48 ms Porb = 1236 d
PSR J2032+4127 Pspin = 143 ms Porb = 16000-17000 d

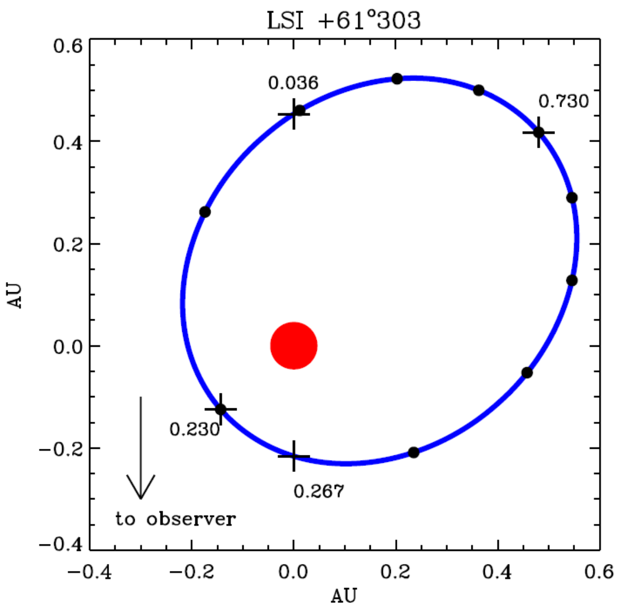

Free-free absorption by stellar wind washes pulsations out

$$\tau_{\rm ff} \approx 14.7\ g_{\rm ff}\left(\frac{\nu}{10^9\ {\rm Hz}}\right)^{-2}\left(\frac{\dot{M}_{\rm w}}{10^{-7}\,M_\odot\,{\rm yr}^{-1}}\right)^{2}\left(\frac{v_{\rm w}}{1000\ {\rm km\,s^{-1}}}\right)^{-2} \times \left(\frac{T_{\rm w}}{10000\ {\rm K}}\right)^{-3/2}\left(\frac{d}{1\ {\rm AU}}\right)^{-3}$$

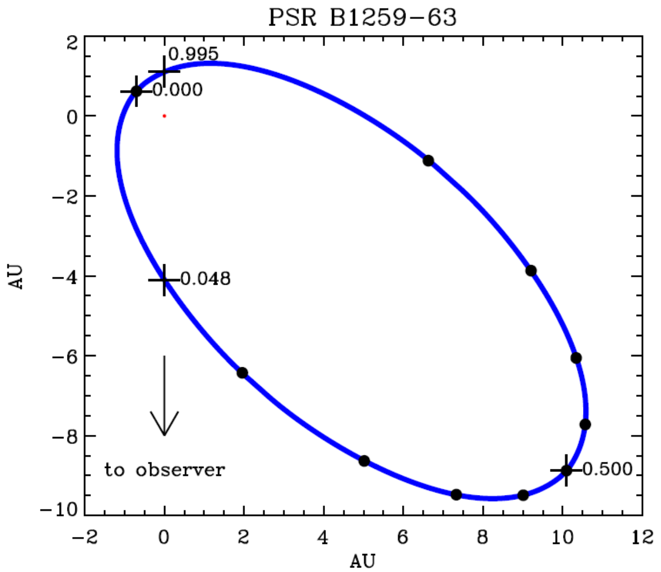

Radio emission changing morphology at different orbital phases. Cometary pulsar nebula tail or a preceding jet?

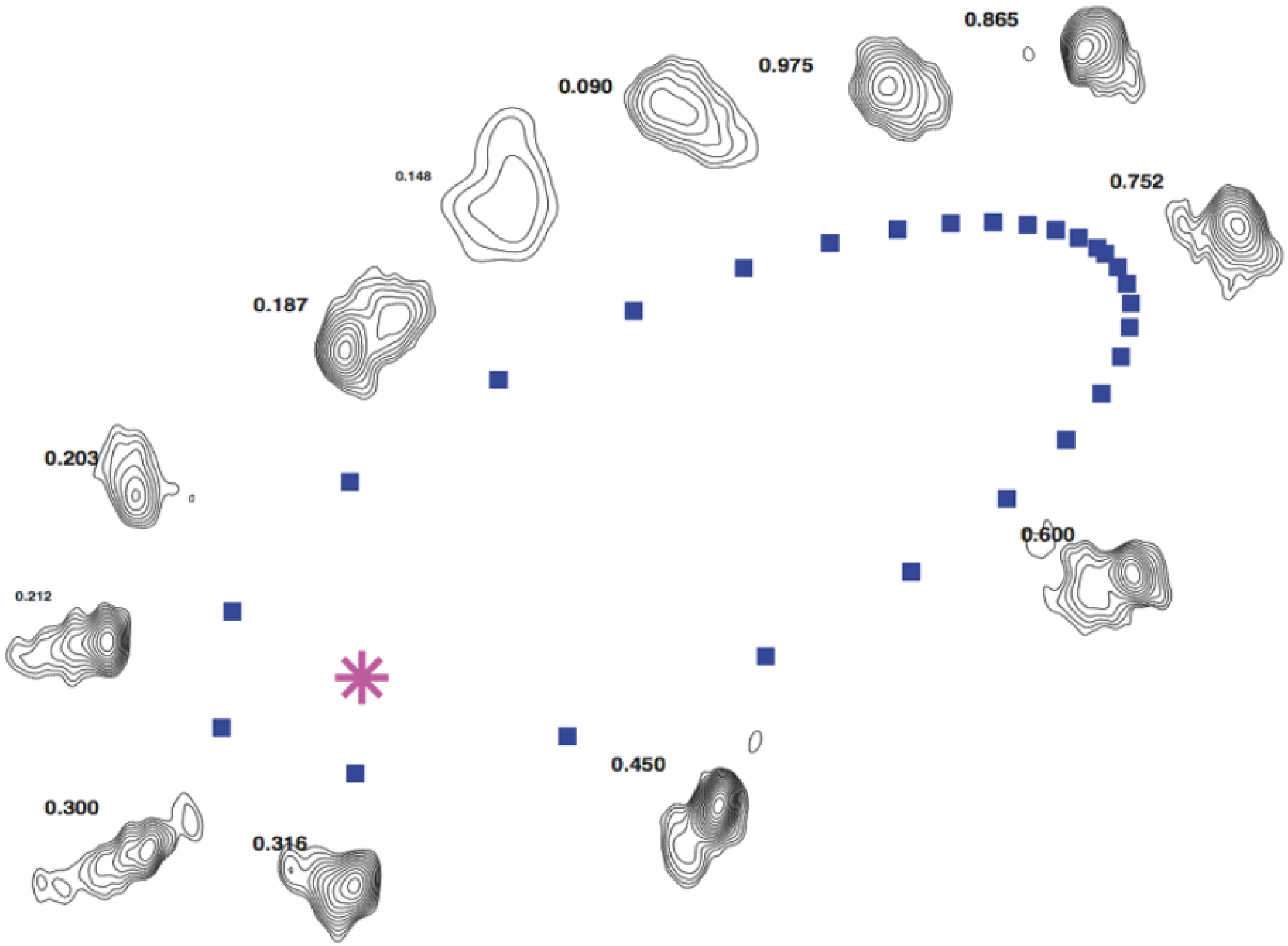

Dhawan+ 2006

A microquasar powering LS I + 61 303? Spectral variability

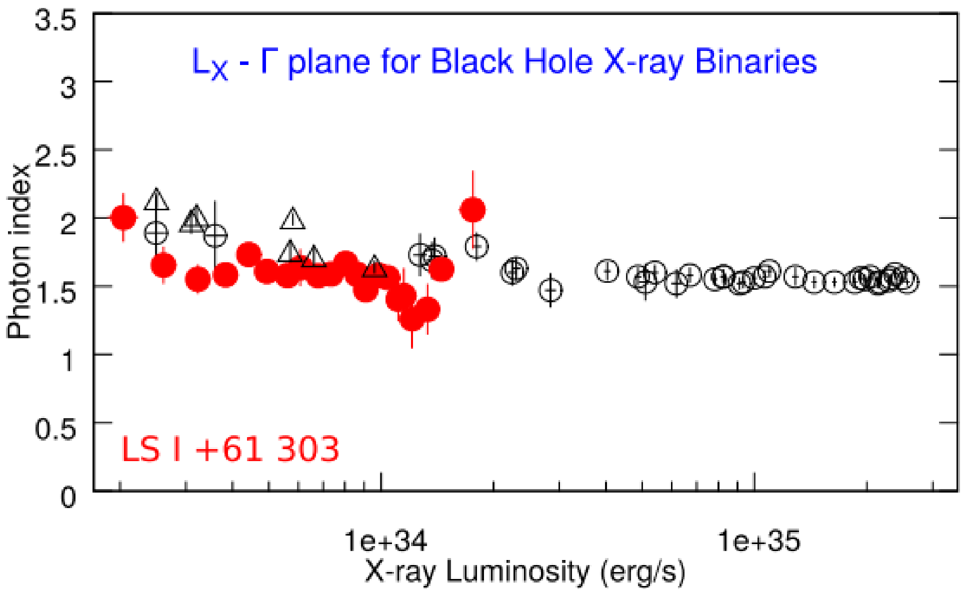

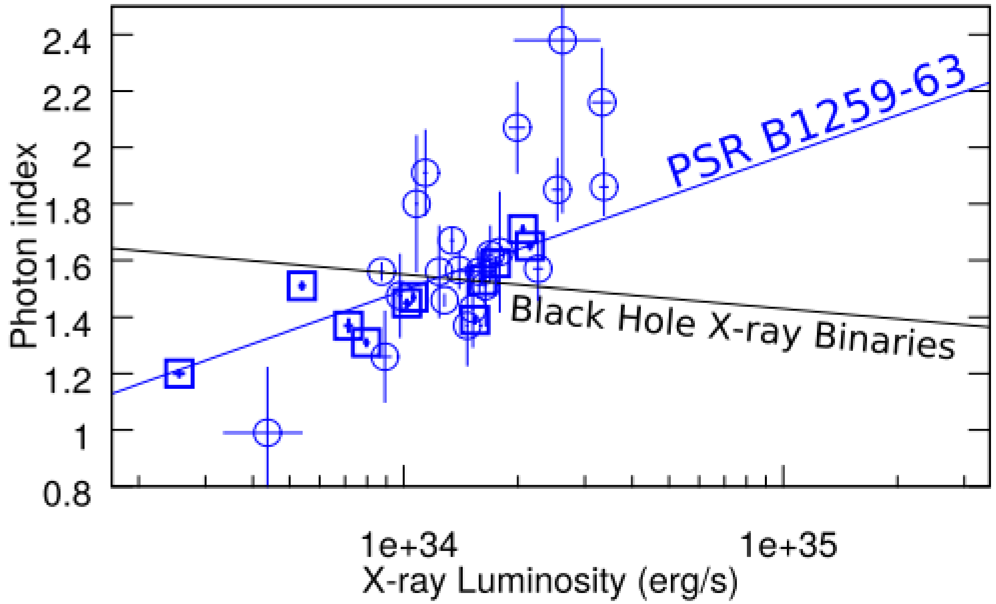

Massi+ 2017

A microquasar powering LS I + 61 303? Temporal variability

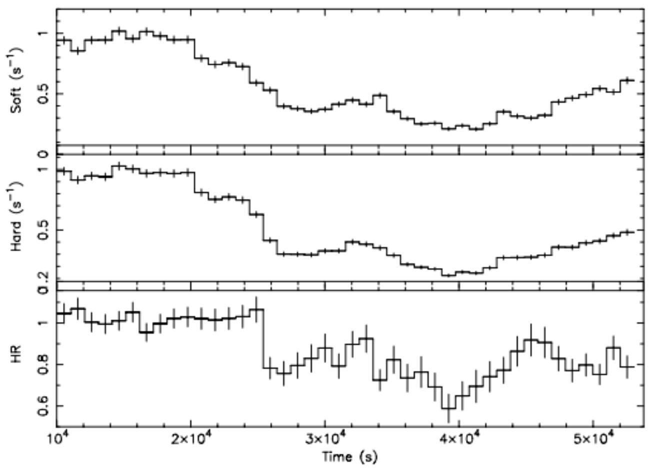

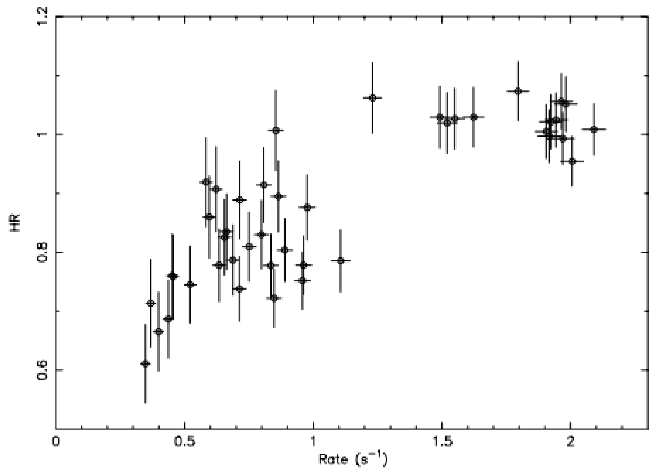

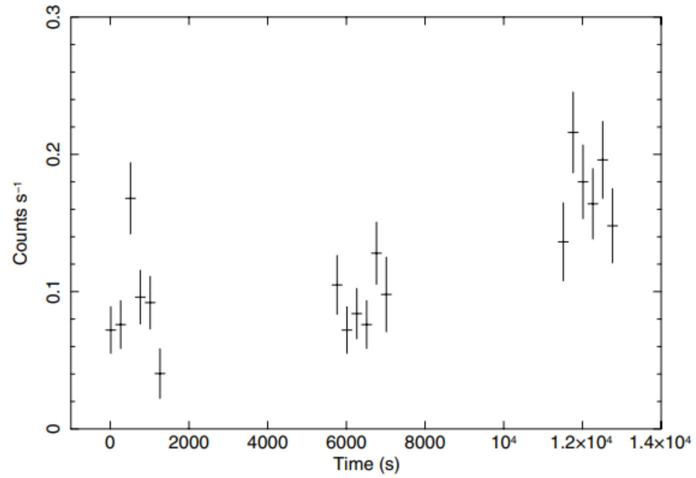

Sidoli+ 2006; Esposito+ 2007

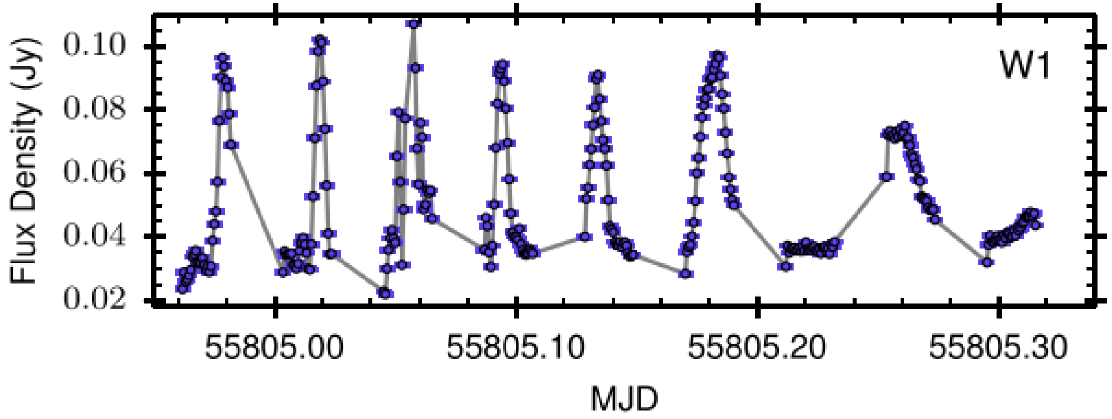

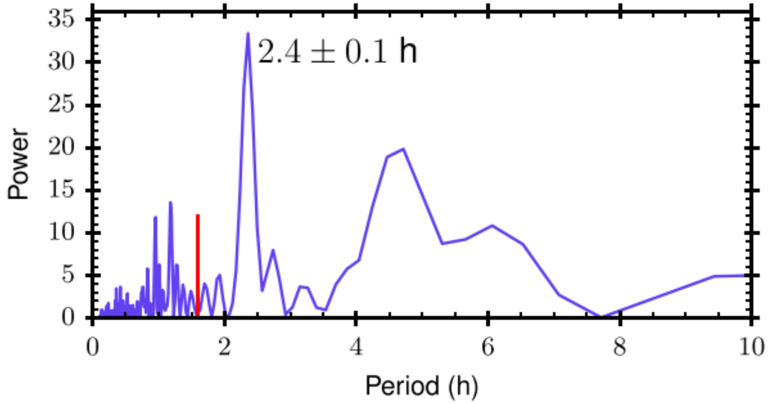

Nösel+ 2017

Magnetar-like bursts from LS I +61 303

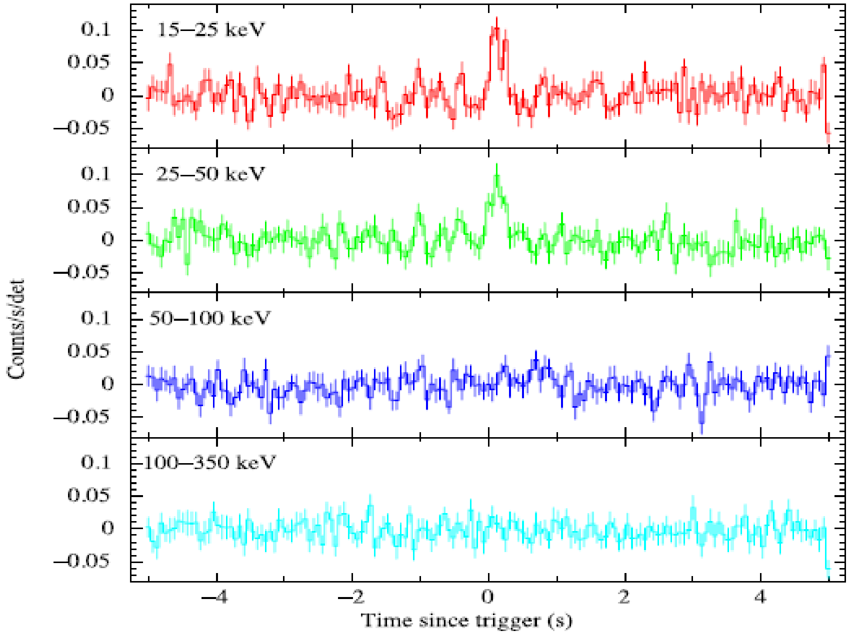

Duration ~ 230 ms
Luminosity ~ 10^{37} (d/2kpc)^2 erg/s
kTbb = (7.0 +/- 0.9) keV
Rbb = (0.27 +/- 0.06) km

De Pasquale+ 2008; Munoz-Arjonilla+ 2009; Torres, Rea+ 2012

No other candidate X-ray counterparts in CXO image

Probability to find a magnetar by chance within 1.4′ ~ 10^{-5}

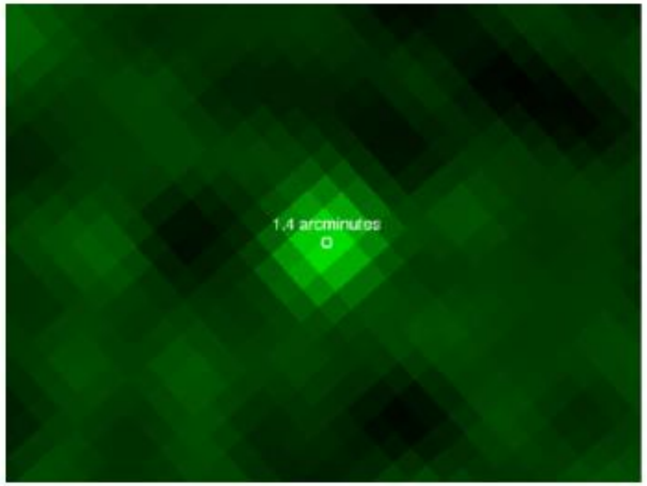

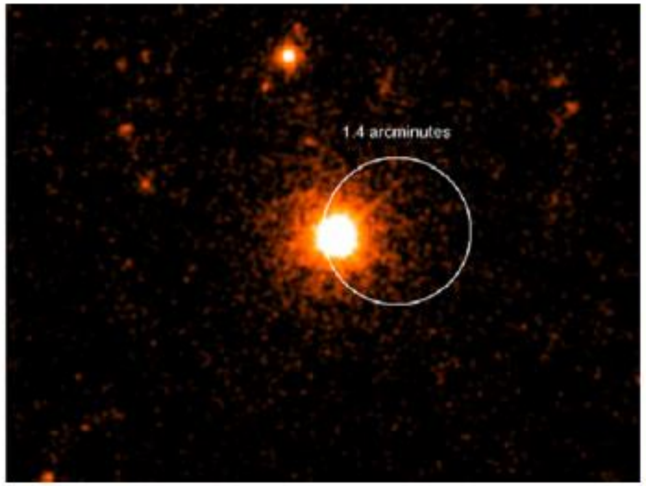

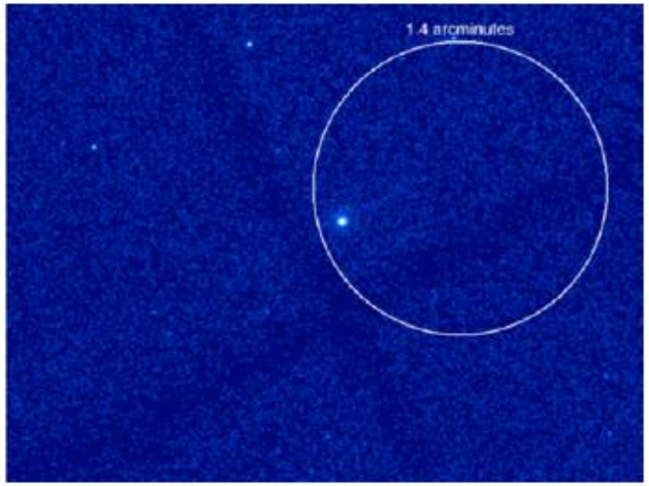

The 500-m Aperture Spherical radio Telescope (FAST)

Largest single dish radio telescope in the world

Sperical reflector – radius 300m, aperture 500m

L-band (1.05-1.45 GHz) 19-beam array receiver

nature astronomy

LETTERS

https://doi.org/10.1038/s41550-022-01630-1

Check for updates

Radio pulsations from a neutron star within the gamma-ray binary LS I +61° 303

Shan-Shan Weng[1,14] ✉, Lei Qian[2,3,14], Bo-Jun Wang[2,4,5,14], D. F. Torres[6,7,8] ✉, A. Papitto[9], Peng Jiang[2,3], Renxin Xu[4,5], Jian Li[10,11], Jing-Zhi Yan[12], Qing-Zhong Liu[12], Ming-Yu Ge[13] and Qi-Rong Yuan[1]

2020 January, 7 (exposure 3 hours)

P = 269.15508(16) ms

DM =240.1pc/cm^3

Significance 22.4 σ

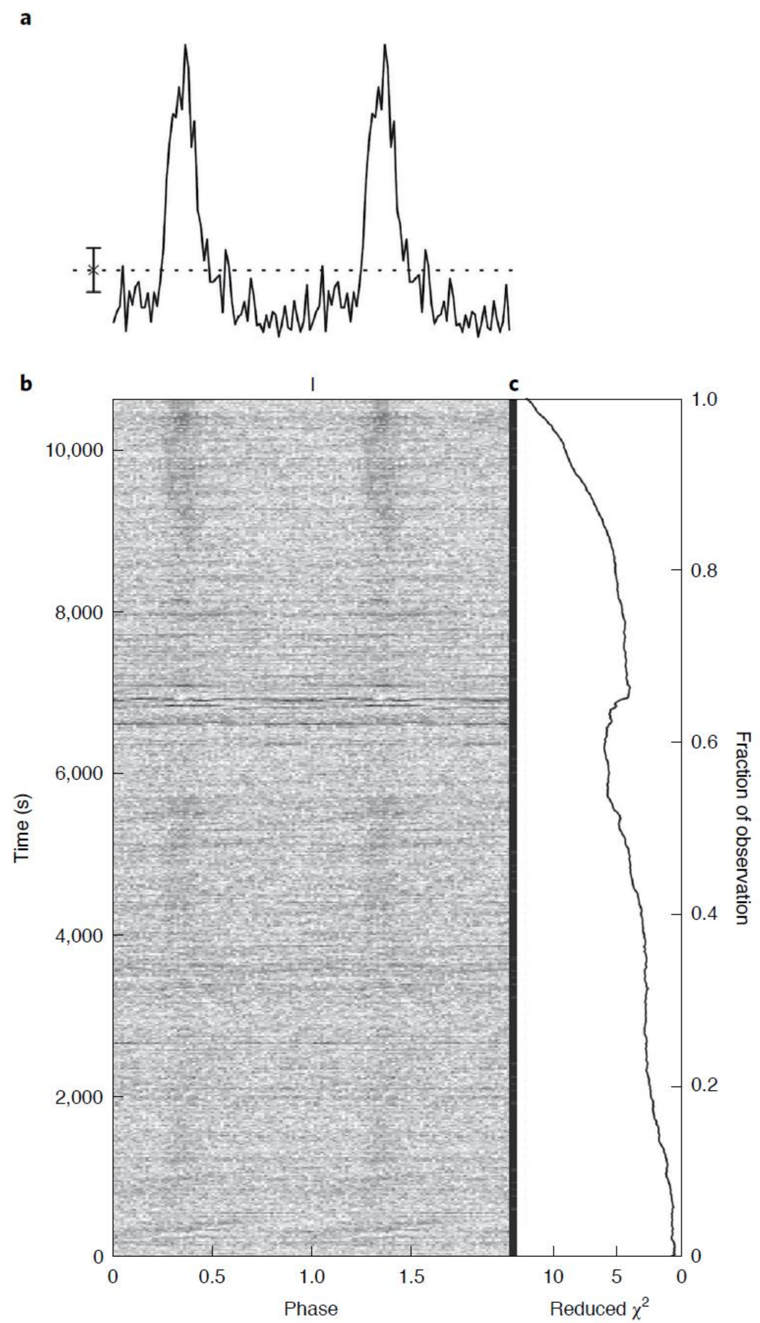

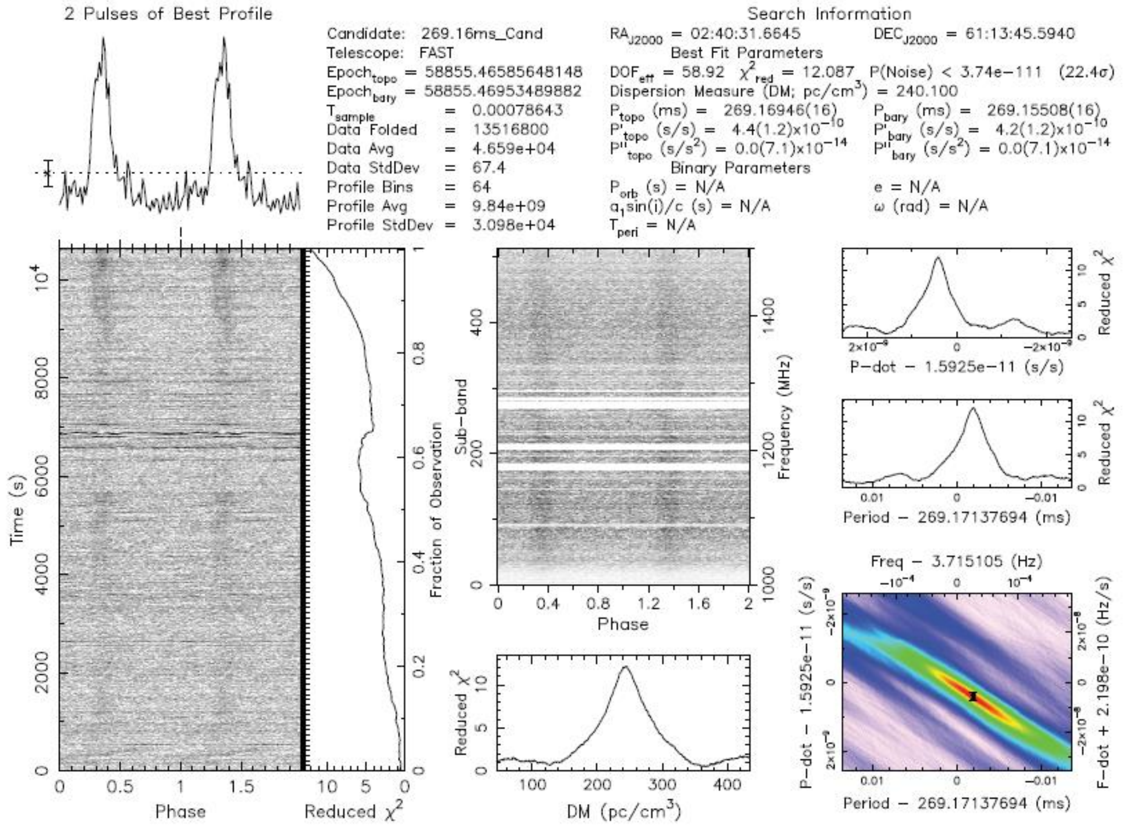
2 Pulses of Best Profile
Search Information
Candidate: 269.16ms_Cand
Telescope: FAST
Epoch_topo = 58855.46585648148
Epoch_bary = 58855.46953489882
T_sample = 0.00078643
Data Folded = 13516800
Data Avg = 4.659e+04
Data StdDev = 67.4
Profile Bins = 64
Profile Avg = 9.84e+09
Profile StdDev = 3.098e+04
RA_J2000 = 02:40:31.6645
DEC_J2000 = 61:13:45.5940
Best Fit Parameters
DOF_eff = 58.92 χ²_red = 12.087 P(Noise) < 3.74e−111 (22.4σ)
Dispersion Measure (DM; pc/cm³) = 240.100
P_topo (ms) = 269.16946(16)
P_bary (ms) = 269.15508(16)
P'_topo (s/s) = 4.4(1.2)x10⁻¹⁰
P'_bary (s/s) = 4.2(1.2)x10⁻¹⁰
P''_topo (s/s²) = 0.0(7.1)x10⁻¹⁴
P''_bary (s/s²) = 0.0(7.1)x10⁻¹⁴
Binary Parameters
P_orb (s) = N/A
e = N/A
a₁sin(i)/c (s) = N/A
ω (rad) = N/A
T_peri = N/A
Time (s)
Phase
Reduced χ²
Fraction of Observation
Sub-band
Frequency (MHz)
DM (pc/cm³)
P-dot − 1.5925e-11 (s/s)
Period − 269.17137694 (ms)
Freq − 3.715105 (Hz)
F-dot + 2.198e-10 (Hz/s)

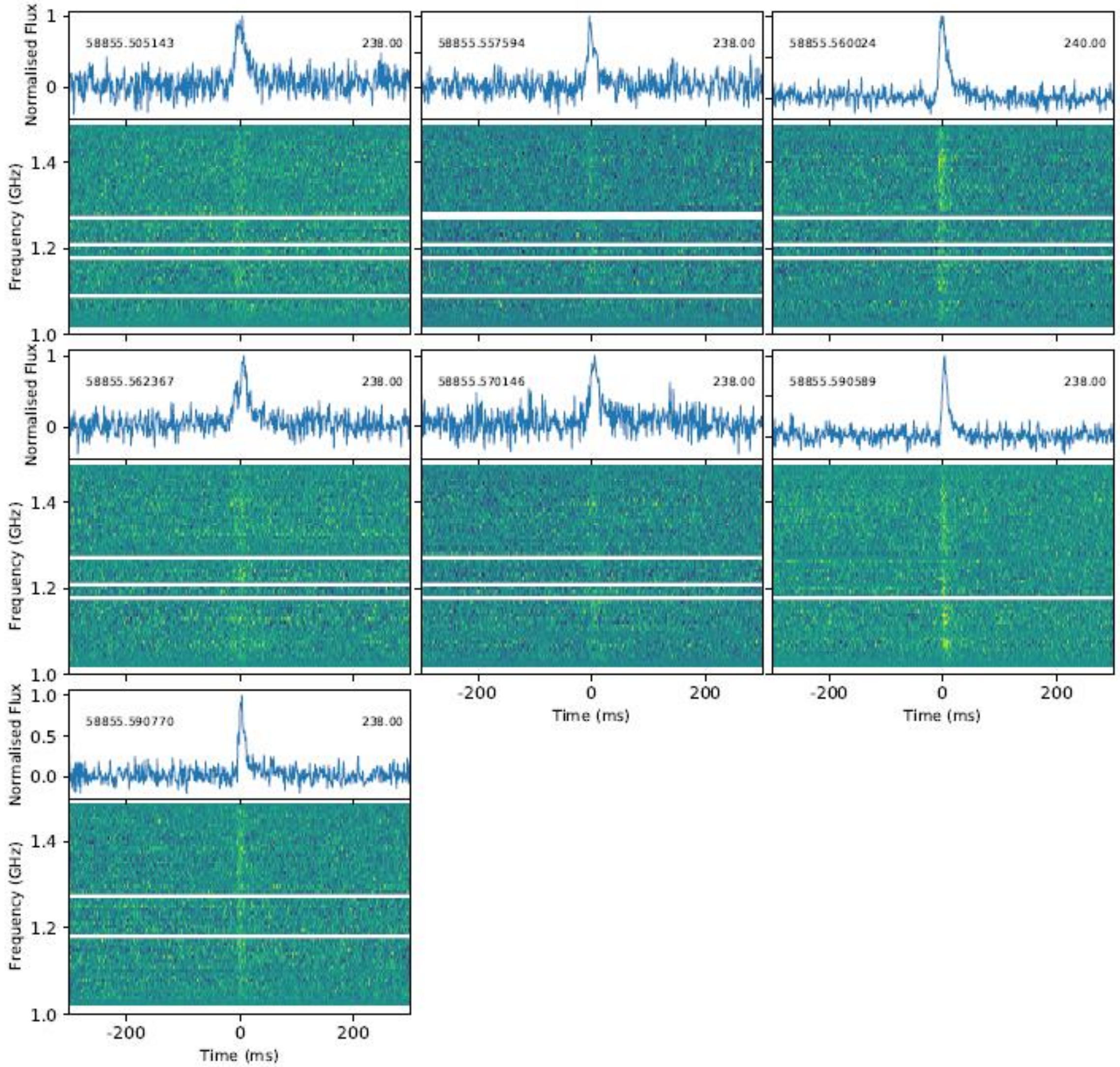
Normalised Flux
Frequency (GHz)
Time (ms)
58855.505143 238.00
58855.557594 238.00
58855.560024 240.00
58855.562367 238.00
58855.570146 238.00
58855.590589 238.00
58855.590770 238.00

Table 1 | Observational log

Middle of observation time	Orbital phase	Exposure time (h)	Sampling time (μs)	Pulse detected	S_{mean} (μJy)	S_{UL} (μJy)
58,788.7257	0.07	2.2	98.304	No	–	1.61
58,855.5278	0.59	3.0	98.304	Yes	4.40	1.37
59,093.8646	0.58	3.0	196.608	No	–	1.37
59,094.8681	0.62	2.0	196.608	No	–	1.68

The orbital phases are calculated with the radio ephemeris given in ref. [3]. S_{mean}, mean flux density for detection; S_{UL}, upper limit of the flux density; –, mean flux density for non-detection.

$$S_{\rm mean} = \frac{\eta\beta T_{\rm sys}}{G\sqrt{N_{\rm p}\Delta\nu T_{\rm int}}}\sqrt{\frac{W}{P-W}}$$

<u>**Antenna gain:**</u>

FAST G = 16 K/Jy

GBT (64m)/Effelsberg (100m) G=1.55/2 K/Jy

-> 20/30 hours would have been needed for a detection

Previous upper limits: 4-15 μJy (1.6-9.3 GHz)
McSwain+ 2011, Cañellas+ 2012

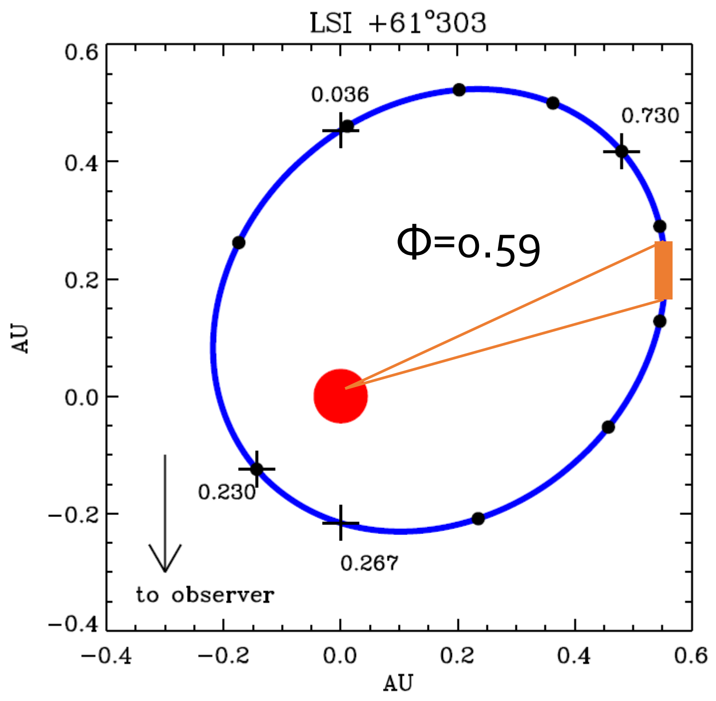

Table 1 | Observational log

Middle of observation time	Orbital phase	Exposure time (h)	Sampling time (μs)	Pulse detected	S_{mean} (μJy)	S_{UL} (μJy)
58,788.7257	0.07	2.2	98.304	No	–	1.61
58,855.5278	0.59	3.0	98.304	Yes	4.40	1.37
59,093.8646	0.58	3.0	196.608	No	–	1.37
59,094.8681	0.62	2.0	196.608	No	–	1.68

The orbital phases are calculated with the radio ephemeris given in ref. [3]. S_{mean}, mean flux density for detection; S_{UL}, upper limit of the flux density; –, mean flux density for non-detection.

An additional detection at phase 0.69, but signal mostly absent

Interstellar scintillation produces changes over a few minutes

Pulsar nulling/mode changing?
(but usually from older/slower pulsars)

Clumpiness of Be stellar wind (Zdziarski+ 2010)

Variations on minutes/hours observed from PSR B1259-63
(Johnston+ 2005)

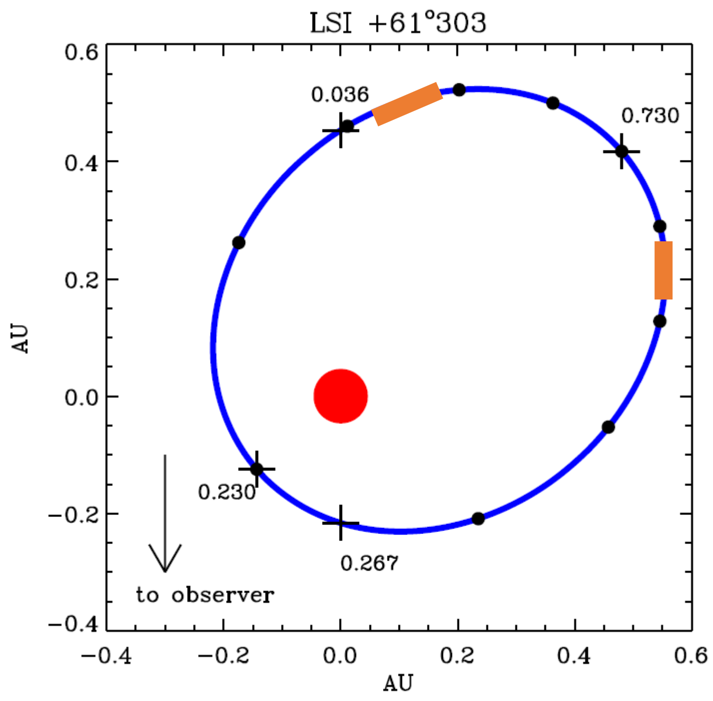

Is LS I +61 303 the source of radio pulsations/magnetar bursts?

Radio pulsar position uncertainty = 2.9′

Magnetar burst position uncertainty = 1.4′

Radio pulsar surface density (|b|< 10°) ~ 8 x 10^{-5} arcmin^{-2}

Probability of two pulsars in 2.9′ ~ 4 x 10^{-6}
(coincident with a gamma-ray binary <10^{-10})

Simulations of a 2000 magnetar population produce
chance superimposition with p = 0.9 x 10^{-3}

Measuring the **pulsar timing orbital solution** would prove the association even further

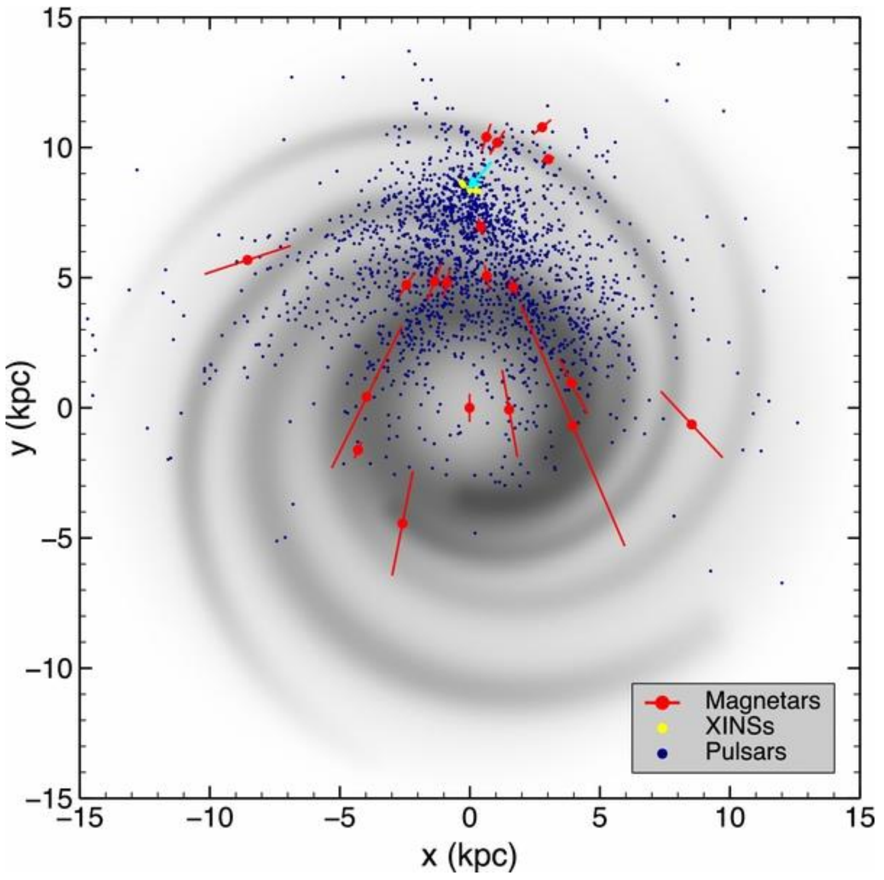

Search for X-ray pulsations in archival data

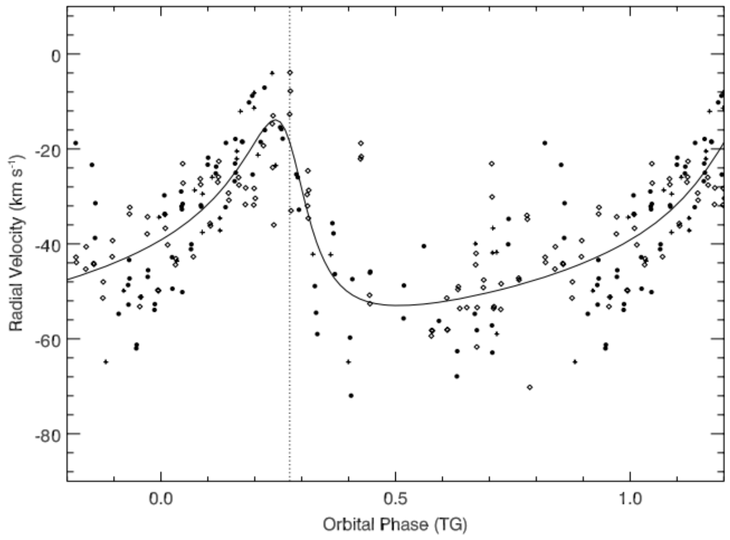

RXTE	940 ls
XMM-Newton	225 ks
Chandra	100 ks
NICER	166 ks

Orbital solution obtained from the donor radial velocity curves
[Casares+ 2005, Aragona+ 2009, Kravtsov+ 2020]

-> **Limited sensitivity** (both frequency range and exposure)

Upper limit Amplitude ~ 5% (**<u>preliminary</u>**)
Previous upper limits 10-15 % [Rea et al. 2012]

Fermi/LAT gamma-ray pulsation search ongoing
[Torres, Papitto, Illiano et al., in prep.]

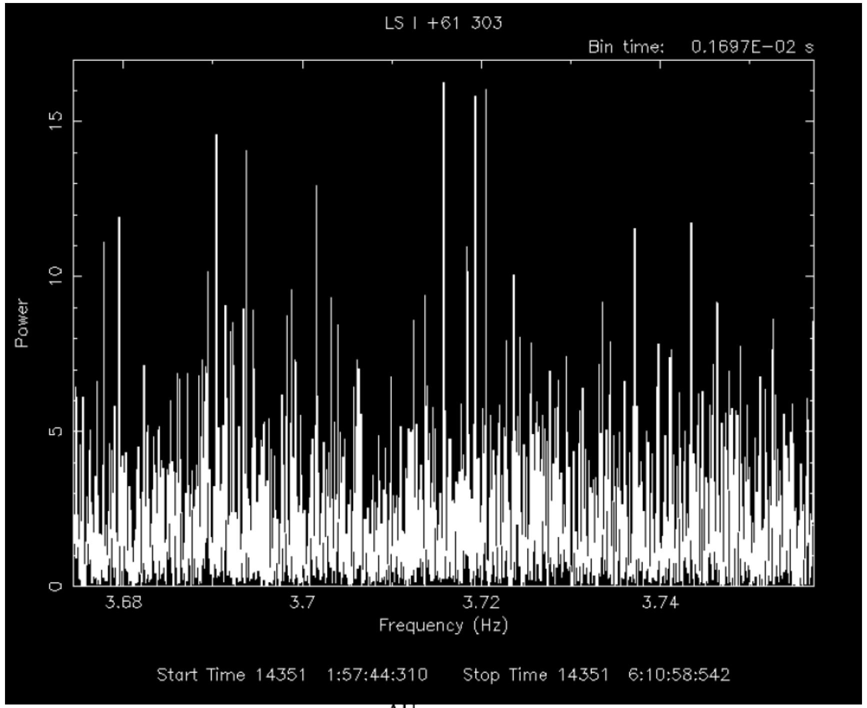

AU

Pulsar states

Increasing Mass Accretion Rate

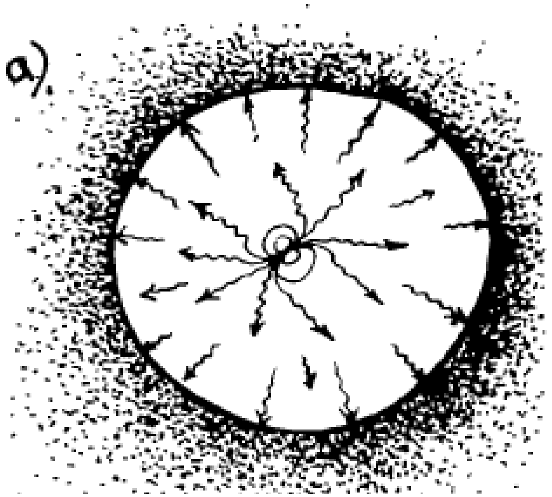

Ejector

Radio/gamma-ray pulsar

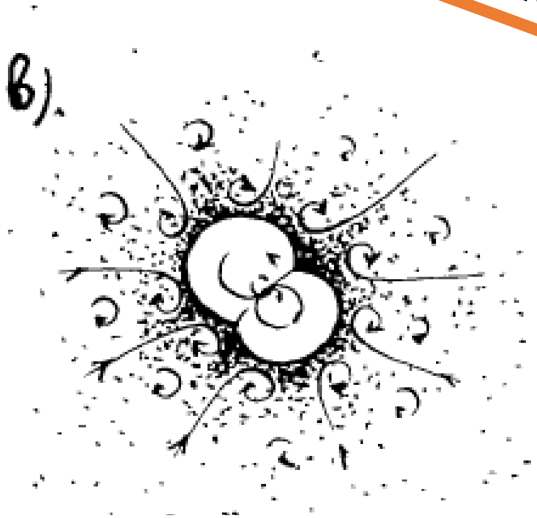

Propeller

Weak X-ray source
High energy source?

Accretor

X-ray pulsar
No high energy emission

Flip-flop model for LS I +61 303

Pulsar works as an ejector at apastron and as a propeller at periastron
[Gnusareva & Lipunov 1985, Stella et al. 1986; Campana et al. 1995]

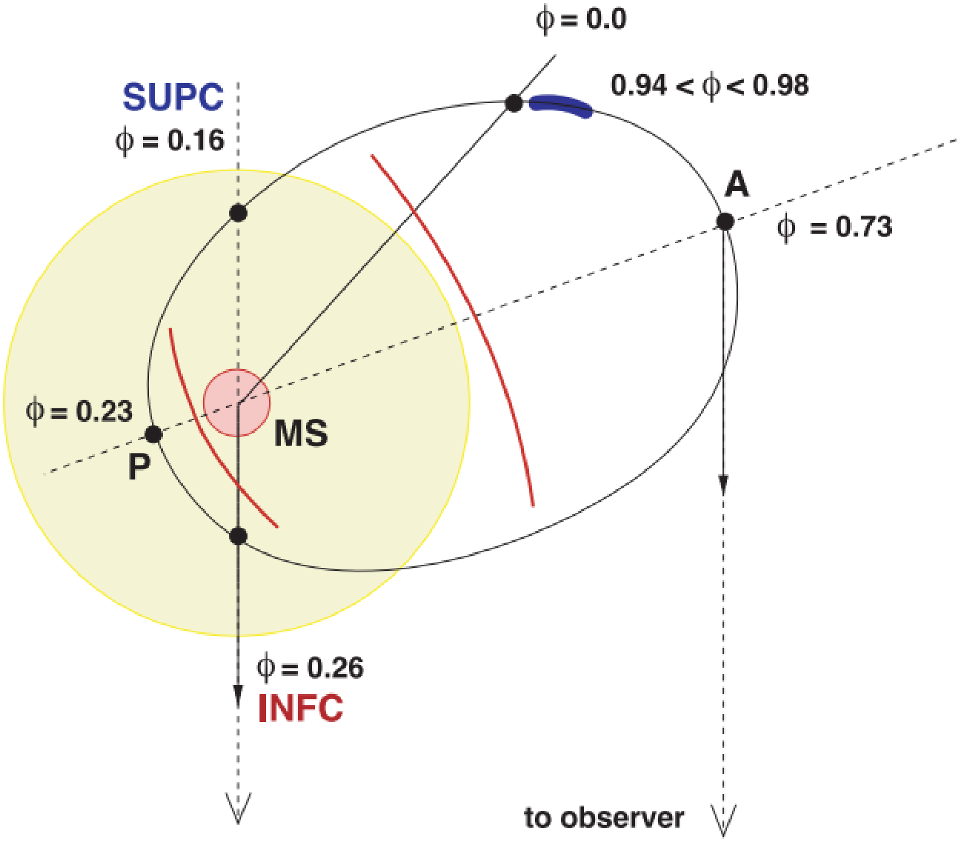

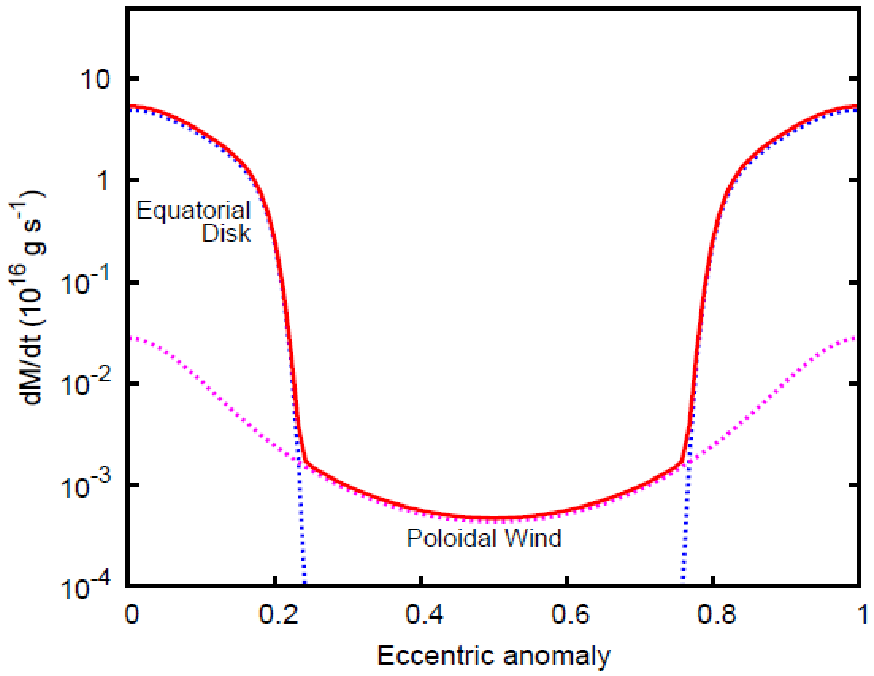

Flip-flop model for LS I +61 303

$$E_{\rm max} \approx 60\xi^{-1/2}\left(\frac{1\ {\rm G}}{B}\right)^{1/2}\ {\rm TeV}$$

Max energy of electrons accelerated in a magnetized shock

(gamma-ray) Pulsar Wind nebula

$$B \approx 1.7\left(\frac{\dot{E}}{10^{37}\ {\rm erg\ s^{-1}}}\right)^{1/2}\left(\frac{\sigma}{10^{-3}}\right)^{1/2}\left(\frac{10^{12}\ {\rm cm}}{R_s}\right){\rm G}$$

propeller

$$B(R) = B_{ns}\left(\frac{R_{ns}}{R}\right)^3$$

As high as 10^{3-4} G for Bns 10^{13-14} G

TeV emission peaks at apastron;
GeV emission peaks at periastron
[Torres+ 2012]

Superorbital variability dictated by oscillation of the Be star decretion disc [Ackermann+ 2013]

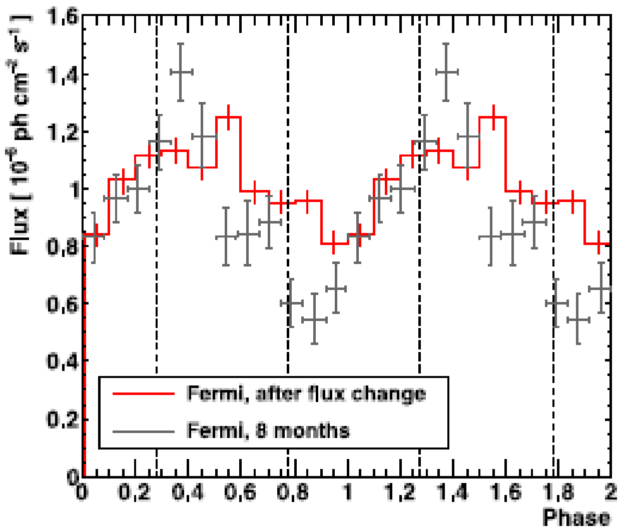

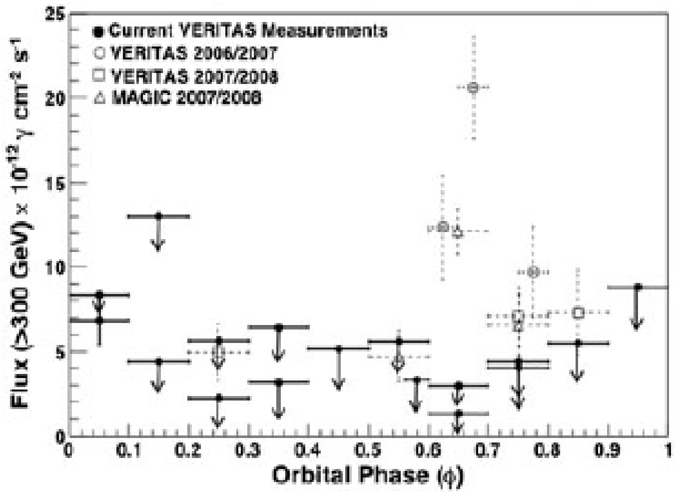

Flip-flop model for LS I +61 303

PSR wind pressure $B^2 P^{-4}$

Accretion prevented as long as:

$P < 0.24\ (B/10^{13}G)^{4/7}\ (\dot{M}/10^{17}g/s)^{-2/7}$
[Papitto+ 2013]

The observed period (0.27 s) is just within the flip-flop interval

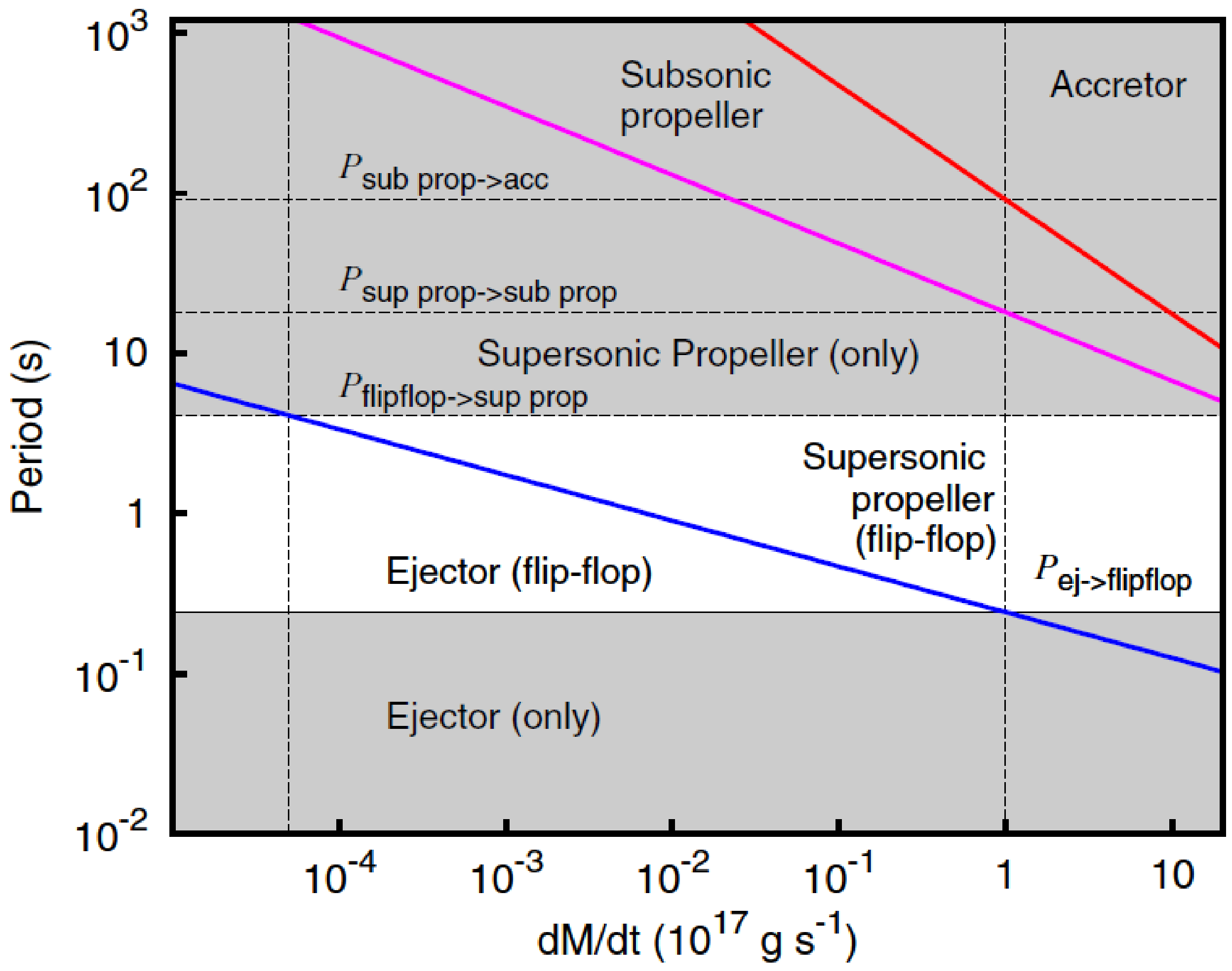

Flip-flop model for LS I +61 303

$Time_{flip\text{-}flop}/Time_{PSR} \sim 4\ (B/10^{13}G)^{-0.24}\ (\dot{M}/10^{17}g/s)^{0.27}$

For short orbital periods (<30d), a gamma-ray binary is most likely found in a flip-flop phase

In larger systems (>100d), the ejector phase is longer

For L_{sd} = 5 x 10^{35} erg/s and B=10^{13} G
we expected P=0.26 s

-> remarkably similar to the value later observed!

System age < 10 kyr

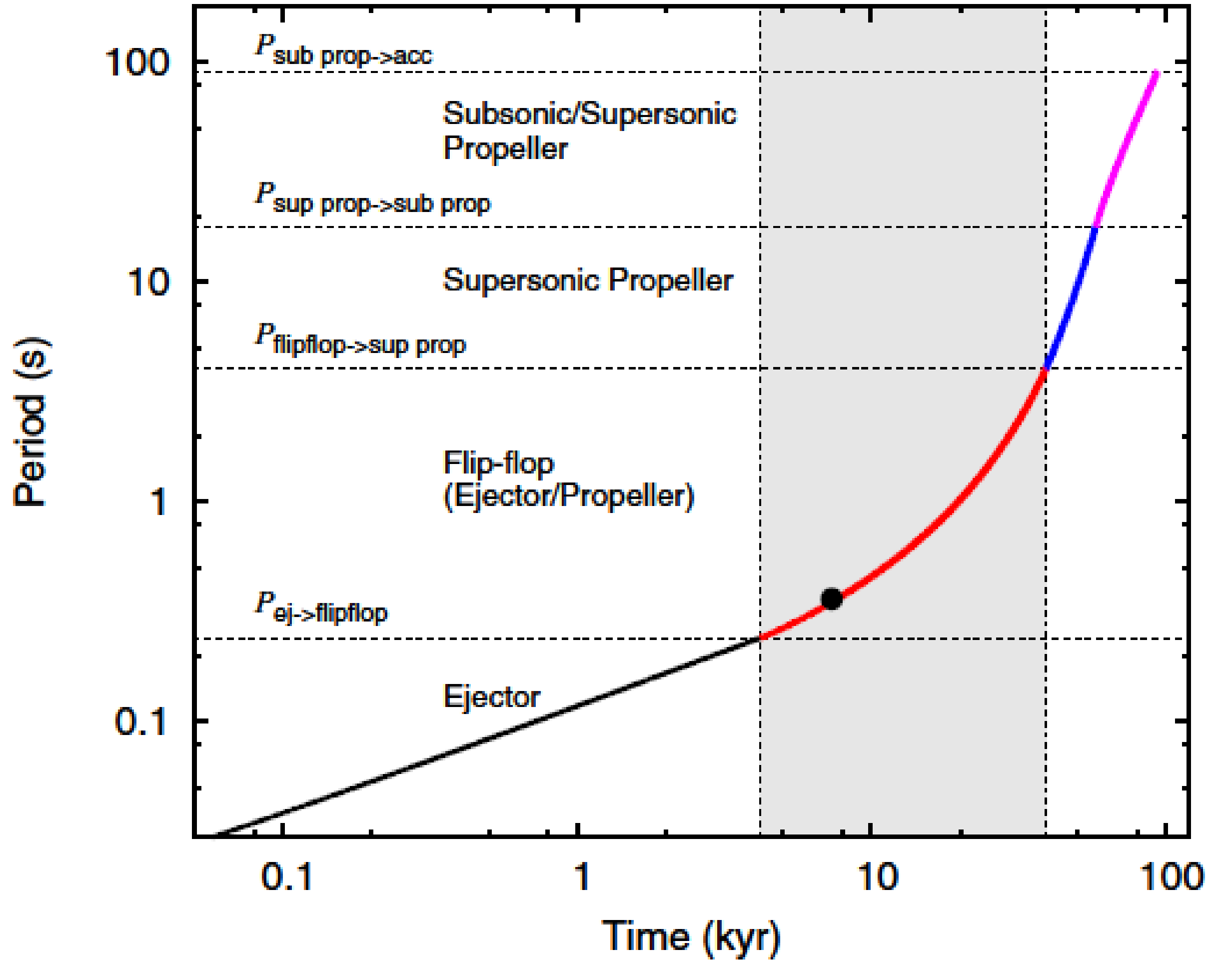

Flip-flop model for LS I +61 303

Assuming the flip-flop state:

Lsd = 10^{35} – a few 10^{36} erg/s

B = a few 10^{12} – 10^{13} G

To work as an ejector in the whole orbit:

- **Higher magnetic fields/spin-down power**
- **Younger age (< 1-2 kyr)**

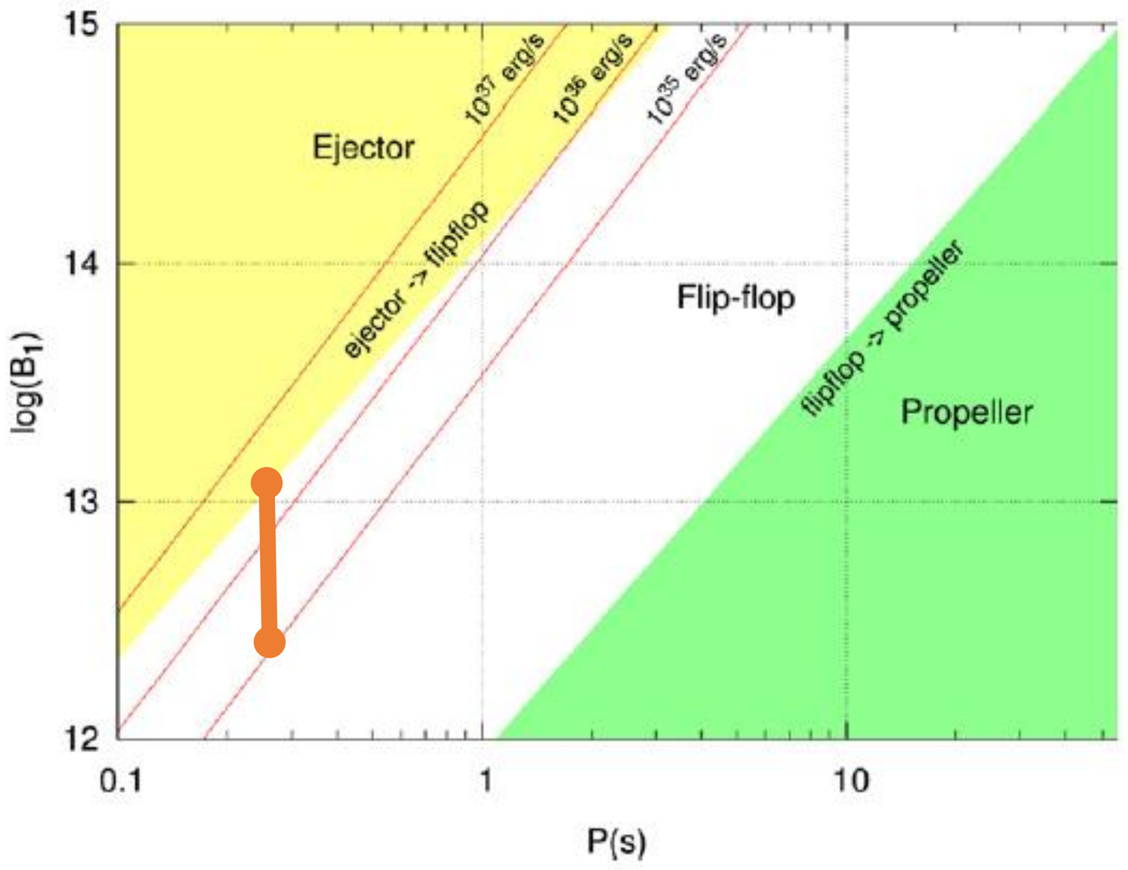

Gamma-ray binaries & ante-diluvian systems

Table 4
Ante-diluvian Systems and LS I +61°303

Name	P_S (s)	P_{orb} (days)	e	B_1[a] (G)	M_2 ($M_\odot$)
J1740−3052	0.57	231.0	0.57	3.9×10^{12}	11.0–15.8
J1638−4725	0.76	1941	0.95	1.9×10^{12}	5.8–8.1
J0045−7319	0.93	51.1	0.81	2.1×10^{12}	3.9–5.3
B1259−63	0.048	1237	0.87	3.3×10^{11}	3.1–4.1
LS I +61°303	···	26.5	0.63	···	10–15

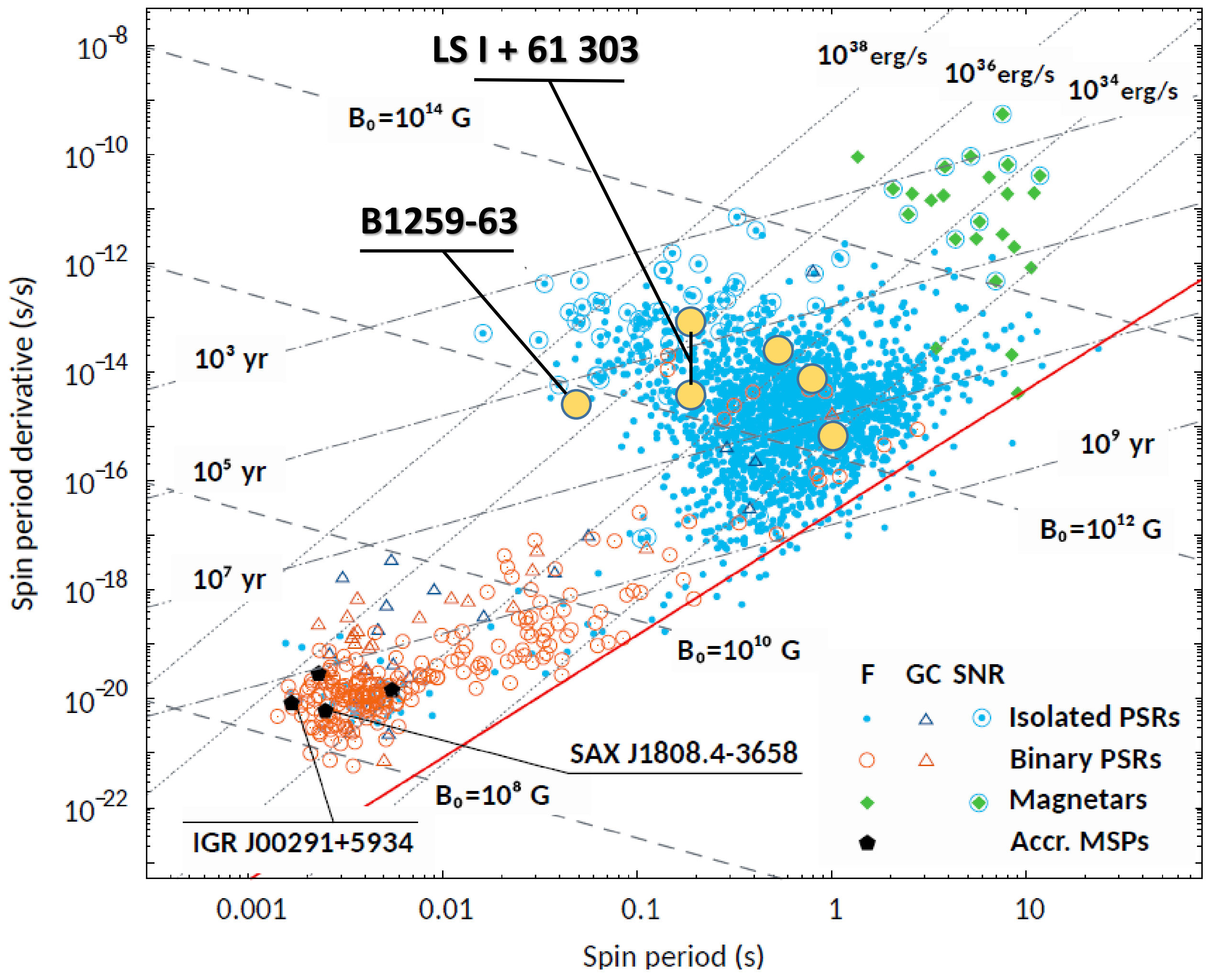

Gamma-ray binaries & HMXBs

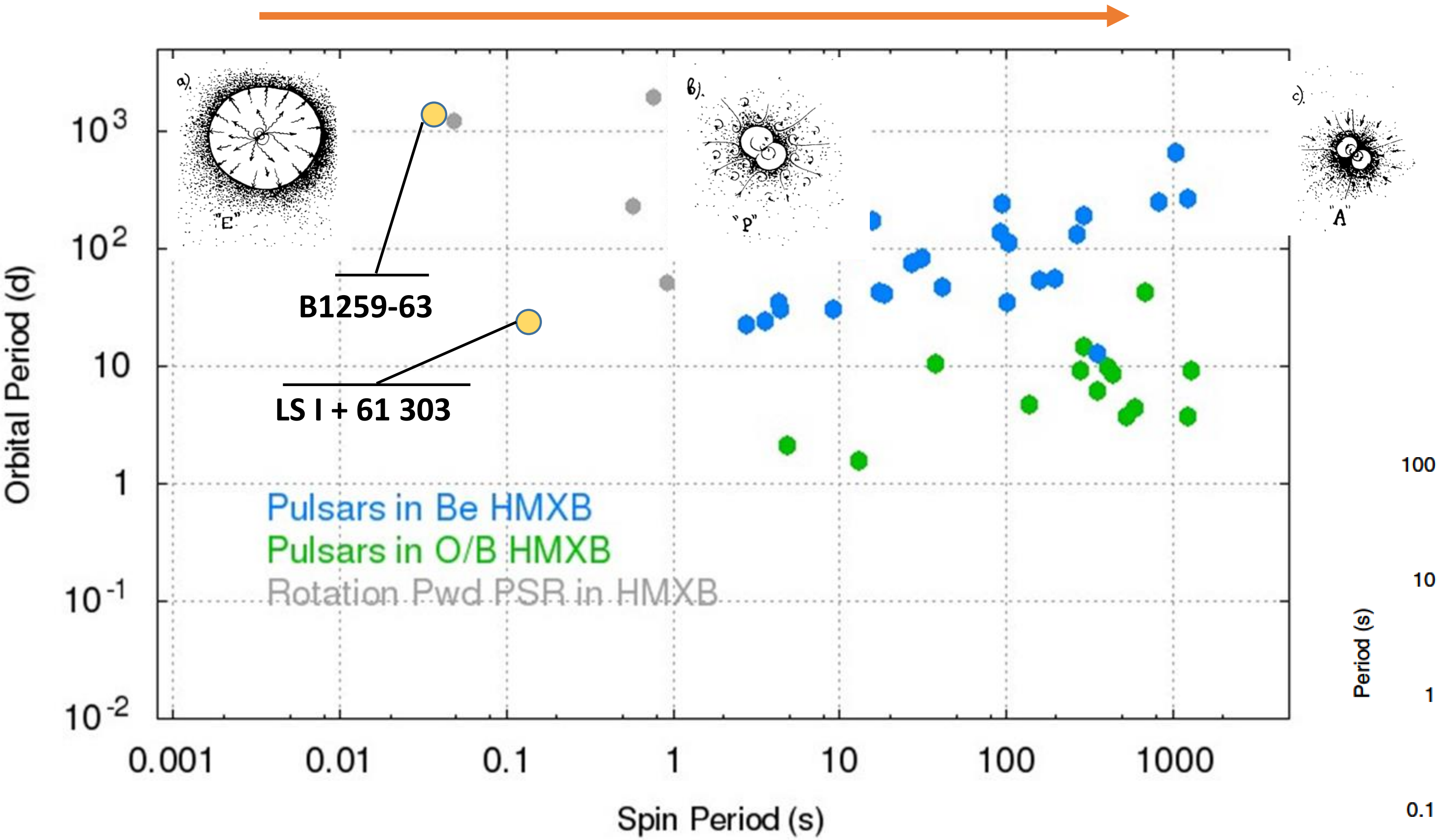

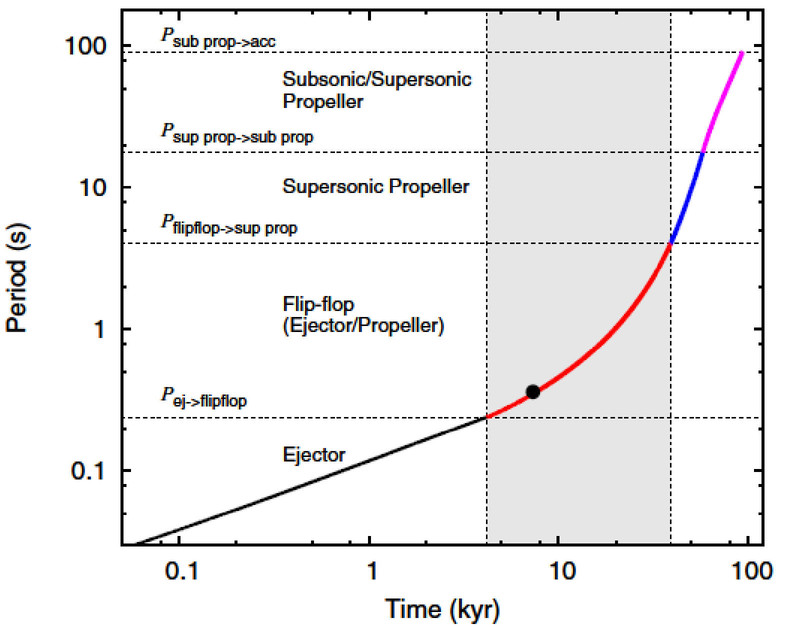

Pulsar interpretation of gamma-ray binaries

Three (out of eight) are pulsars

Spectral and timing characteristics are similar for all systems

Pulsar wind nebulae are the most common Galactic HE/VHE sources

Magnetar bursts from LS I + 61 303

HE spectrum with an exponential cut-off

nature astronomy
LETTERS
https://doi.org/10.1038/s41550-022-01630-1

Check for updates

Radio pulsations from a neutron star within the gamma-ray binary LS I +61° 303

Shan-Shan Weng[1,14] ✉, Lei Qian[2,3,14], Bo-Jun Wang[2,4,5,14], D. F. Torres[6,7,8] ✉, A. Papitto[9], Peng Jiang[2,3], Renxin Xu[4,5], Jian Li[10,11], Jing-Zhi Yan[12], Qing-Zhong Liu[12], Ming-Yu Ge[13] and Qi-Rong Yuan[1]

LS I +61° 303 hosts a **young, highly magnetised NS with magnetar behavior**

Gamma-ray binaries are **pulsar wind nebulae in a binary environment**

Gamma-ray binaries are **progenitors of high mass X-ray binaries**